

**CHIP SEALS FOR ASPHALT CONCRETE PAVEMENTS:  
A PROPOSED EMULSION RESIDUE SPECIFICATION AND  
EXISTING PAVEMENT TEXTURE EVALUATION**

A Thesis

by

DENISE MARIE HOYT

Submitted to the Office of Graduate Studies of  
Texas A&M University  
in partial fulfillment of the requirements for the degree of

MASTER OF SCIENCE

May 2012

Major Subject: Civil Engineering

Chip Seals for Asphalt Concrete Pavements:  
A Proposed Emulsion Residue Specification and Existing Pavement Texture Evaluation  
Copyright 2012 Denise Marie Hoyt

**CHIP SEALS FOR ASPHALT CONCRETE PAVEMENTS:  
A PROPOSED EMULSION RESIDUE SPECIFICATION AND  
EXISTING PAVEMENT TEXTURE EVALUATION**

A Thesis

by

DENISE MARIE HOYT

Submitted to the Office of Graduate Studies of  
Texas A&M University  
in partial fulfillment of the requirements for the degree of

MASTER OF SCIENCE

Approved by:

Chair of Committee,	Amy Epps Martin
Committee Members,	Robert L. Lytton
	Charles Glover
Head of Department,	John Niedzwecki

May 2012

Major Subject: Civil Engineering

## ABSTRACT

Chip Seals for Asphalt Concrete Pavements: A Proposed Emulsion Residue Specification and Existing Pavement Texture Evaluation. (May 2012)

Denise Marie Hoyt, B.S., Texas A&M University

Chair of Advisory Committee: Dr. Amy Epps Martin

Chip seals are a pavement surface treatment used for maintaining asphalt concrete pavements. National Cooperative Highway Research Program (NCHRP) Project 14-17 was performed to produce a national Chip Seal Manual which would consolidate the best chip seal engineering practices. A subcontract to NCHRP Project 14-17 performed at Texas A&M University was the basis for this thesis. It included the following tasks: investigation of a testing and grading system for grading asphalt binder residues from chip seal emulsions; and investigation of texture measurement methods for assessing existing pavement macrotexture before a chip seal is placed.

The performance graded (PG) asphalt binder specification, which was developed to characterize asphalt binder properties related to the performance of hot mix asphalt concrete in pavements, cannot be directly applied to asphalt binders or emulsion residues for use in chip seals. Therefore, the surface performance graded (SPG) specification was developed using the same equipment as the PG system but with some procedural modifications and different limiting values for the test parameters. NCHRP Project 14-17 utilized the PG and SPG systems to grade base asphalt binders and recovered emulsion residues. Two emulsion residue recovery methods were compared: hot oven evaporation with nitrogen blanket and stirred can with nitrogen purge. The PG and SPG grades were found to be similar for the two emulsion residue recovery methods but slightly different from the base asphalt binder. A strawman specification for emulsion residues in chip seals was recommended for use with the stirred can recovery method.

In chip seal construction, macrotexture of the existing pavement affects the rate at which chip seal emulsion must be applied. In this project, existing pavement

macrotextures were measured at three chip seal projects immediately before construction using both the sand patch test and the circular track meter, CT Meter. The CT Meter was found to quickly and effectively measure pavement macrotexture. The CT Meter measurements correlated well with the sand patch test measurements.

Finally, this project investigated the utility of measuring pavement macrotexture in the laboratory using the aggregate imaging system (AIMS) on pavement cores and on small samples cut from fabricated slabs. Statistical analyses showed good correlation between the mean profile depth, MPD, calculated from AIMS measurements on pavement cores and small samples, based on analysis using 50 mm (2 inch) segment lengths, and the MPD measured on the pavement or on the large fabricated slabs with the CTMeter. These results supported the use of AIMS to measure pavement macrotexture using small samples in the laboratory.

## **DEDICATION**

I dedicate this thesis to Dr. Wiley D. Cunagin and to Charles and Therese Rausch, who each and all believed that I could accomplish whatever I set my mind to doing.

I also dedicate this thesis to Dr. Robert L. Lytton, who encouraged me into and through this masters' degree program twice.

## ACKNOWLEDGEMENTS

Many acknowledgements and thanks are due to the following contributors to this thesis.

I am very grateful to Dr. Amy Epps Martin at Texas A&M University, my advisor and committee chairwoman, who gave me a great amount of guidance and encouragement, and who set an example for me every day. I also am very grateful to Dr. Robert Lytton and Dr. Charles Glover at Texas A&M University, my committee members, who gave graciously and generously of their valuable time and wise guidance. I am proud to have each of their names on my thesis.

Many thanks are due to the National Cooperative Highway Research Program, NCHRP, and especially to Mr. Amir Hanna for sponsoring NCHRP Project 14-17.

I also would like to thank Dr. Scott Shuler at Colorado State University, the Principal Investigator on NCHRP Project 14-17. Dr. Shuler was “around” for my M.S. degree work both times, and he taught me to approach life and work with humor and with an eye to practicality.

Thank you also to Nikornpon Prapaitrakul, Rongbin Han, Xin Jin, and Dr. Charles J. Glover of the Artie McFerrin Department of Chemical Engineering, Texas A&M University, for their untiring and patient work on the emulsion residue recovery, the gel permeation chromatography (GPC), and the Fourier transform infrared (FT-IR) spectroscopy.

I would like to gratefully acknowledge the help given to me by my field work partners, Jim Lawrence and Arash Rezaei. Jim and Arash each worked tirelessly and very carefully, and their company made the field work much more interesting and pleasant.

I also gratefully acknowledge the work of the McNew Laboratory technicians. Rick Canatella and David Zeig taught me to “follow the procedures” and they stimulated much interesting discussion on many topics, including asphalt behavior and life.

I also would like to thank the Texas Transportation Institute, TTI, for allowing us the use of the AIMS equipment. In particular, thanks go to Emad Kassem, manager of the ACIM Laboratory, and to Leslie Gates and the AIMS student workers.

Past support from the Texas Department of Transportation (TXDOT) is gratefully acknowledged. Pavement cores and texture data from TXDOT Project 0-5627, Predicting Asphalt Mixture Skid Resistance Based on Aggregate Characteristics, were used in this study.

Last but not least, I wish to thank the Utah Arches National Park and the Colorado and Washington State Department of Transportation organizations for allowing this research to be conducted on their chip seal projects, and for setting up excellent traffic control during the field studies which kept us safe on the roadways.



## TABLE OF CONTENTS

	Page
ABSTRACT .....	iii
DEDICATION.....	v
ACKNOWLEDGEMENTS .....	vi
TABLE OF CONTENTS.....	viii
LIST OF FIGURES .....	xii
LIST OF TABLES.....	xv
1. THESIS INTRODUCTION .....	1
Pavement Preservation .....	1
Chip Seals as a Preservation Treatment .....	2
Need for a National Chip Seal Manual.....	2
Thesis Overview.....	3
Thesis Outline .....	3
2. ASPHALT BINDER CHARACTERIZATION AND THE PERFORMANCE GRADED (PG) ASPHALT BINDER SPECIFICATION SYSTEM.....	5
High Temperature Behavior .....	6
Low Temperature Behavior .....	6
Intermediate Temperature Behavior.....	6
Rheology.....	6
Asphalt Binder Grading.....	8
PG Grading for Asphalt Binders .....	8
DSR .....	9
BBR .....	10
SPG Grading for Chip Seal Emulsions .....	12

	Page
3. SURFACE PERFORMANCE-GRADING SYSTEM TO GRADE CHIP SEAL EMULSION RESIDUES.....	13
Introduction.....	13
Motivation.....	13
The Surface Performance-Graded (SPG) Specification.....	14
Objective.....	15
Description of Contents.....	15
Experimental Design of NCHRP 14-17 Binder Characterization.....	15
Materials.....	16
Emulsion Recovery Methods.....	16
Laboratory Tests.....	18
Rheology Tests.....	18
Strain Sweep Tests.....	19
Chemical Tests.....	20
Binder Grading.....	21
Results and Analyses.....	22
DSR Results: High Temperatures.....	22
BBR Results: Low Temperatures.....	22
DSR Results: Intermediate Temperatures.....	22
PG and SPG Grading.....	23
Chemical Analysis Results.....	23
Statistical Analyses Summary.....	24
Strain Sweep Results.....	25
Field Site Assessment After One Year.....	30
Recommendations and Conclusions.....	30
Future Research.....	32
4. EXISTING PAVEMENT TEXTURE EVALUATION FOR USE IN CHIP SEAL EMULSION SPRAY RATE ADJUSTMENT.....	34
Introduction.....	34
Texture Measurement.....	34
Description of the Experiment.....	35
Sand Patch Test.....	36
Circular Texture Meter (CT Meter).....	39

	Page
Calculation of the MPD .....	41
Aggregate Imaging System (AIMS) .....	41
AIMS Texture Analysis Using Greyscale Image Analysis and Wavelet Transforms.....	42
AIMS Texture Analysis Using Height Measurements and Profiling ... Ames Laser Texture Scanner .....	46
Results and Analyses.....	49
Conclusions, Recommendations, and Future Research.....	55
5. A SIMPLE LABORATORY METHOD FOR MEASURING PAVEMENT MACROTEXTURE USING PAVEMENT CORES AND THE AGGREGATE IMAGING SYSTEM (AIMS).....	58
Introduction.....	58
Objective.....	61
Methodology .....	61
Procedure .....	61
Texture Measurement Methods.....	64
Circular Texture Meter (CT Meter) .....	64
Aggregate Imaging System (AIMS) .....	65
Results and Discussion .....	69
Theoretical Background for the AIMS Analysis.....	69
The Relationship Between AIMS (Laboratory) MPD and CT Meter (Field) MPD .....	72
Conclusions.....	78
Future Research.....	79
6. SUMMARY OF CONCLUSIONS, RECOMMENDATIONS, AND FUTURE RESEARCH .....	80
Conclusions and Recommendations: Emulsion Residue Testing and Characterization .....	80
Conclusions and Recommendations: Pavement Macrotecture Evaluation ...	82
Recommended Future Research.....	82
REFERENCES .....	85

Page

VITA..... 93

## LIST OF FIGURES

		Page
Figure 1	Dynamic shear rheometer (DSR) equipment at McNew Laboratory, Texas A&M University. DSR is at the left, and computer screen is at the right. A sample in a mold can be seen on the table in front of the DSR.....	9
Figure 2	Bending beam rheometer (BBR) and computer equipment at McNew Laboratory, Texas A&M University.....	11
Figure 3	Strain sweep results for the stirred can recovery residues.....	27
Figure 4	Sand patch testing for pre-existing pavement macrotexture before chip sealing in Washington state: spreading glass beads into a circle. .	37
Figure 5	Sand patch testing for pre-existing pavement macrotexture before chip sealing in Utah: measuring diameters of the circle of glass beads.....	37
Figure 6	CT Meter taking a macrotexture measurement on a fabricated test slab. CT Meter is connected to the laptop computer at the left for data collection.....	38
Figure 7	A technician setting up the CT Meter in the field.....	39
Figure 8	The eight segments of the CT Meter’s circular profile with direction of traffic shown.....	40
Figure 9	The older version of the AIMS equipment is shown. Note that the table is stationary and the camera lens system moves to scan the sample(s) in a grid pattern.....	45
Figure 10	Technician using the Ames laser texture scanner to measure pavement macrotexture.....	46
Figure 11	Texture measurement results from NCHRP Project 14-17 chip seal	

	Page
<p>sites at Arches National Park, UT; a county road in Frederick, CO; US 101 in Washington state; and 3 fabricated test slabs. Sand patch MTD versus CT Meter MPD data points are plotted for each measurement location.....</p>	50
<p>Figure 12 Texture test results from NCHRP Project 14-17 chip seal sites at Arches National Park, UT; Frederick, CO; Washington state US 101; and 3 fabricated test slabs. Linear regression equation was fitted through the data points as shown. ....</p>	51
<p>Figure 13 Comparison of the regression equation from this project to the regression equations from other research. The regression developed from this project falls among the regressions from other research. ....</p>	53
<p>Figure 14 Texture test results from NCHRP Project 14-17 test slabs: Sand patch MTD plotted versus AIMS texture depth, and linear regression equation fitted through the data points. ....</p>	54
<p>Figure 15 Texture test results from NCHRP Project 14-17 test slabs: CT Meter MPD plotted versus AIMS texture depth, and linear regression equation fitted through the data points. ....</p>	54
<p>Figure 16 Pavement texture wavelengths and their associated tire-pavement interaction effects. ....</p>	59
<p>Figure 17 Fabricated concrete slab with rough surface texture being measured by the CT Meter. The diagram of the circumferential segments into which the data are divided can be seen on the top of the CT Meter. ....</p>	63
<p>Figure 18 Three 15.24 cm x 15.24 cm (6 inches x 6 inches) small slab samples with smooth, medium, and rough (left to right) textures cut from negative-image slabs cast on asphalt concrete pavement surfaces. ....</p>	63
<p>Figure 19 Photograph of the inside of the AIMS system showing the camera lens (top), overhead lighting (middle), and rotating specimen tray (bottom) .....</p>	66

	Page
Figure 20	AIMS grayscale image at zoom level 15.8 on a small slab sample. .... 67
Figure 21	Pavement core during scanning in AIMS..... 67
Figure 22	Layout of the laboratory sample measurement directions..... 68
Figure 23	Sample scanlines (of six inch segment lengths) showing profiles of the three different textures from the small slab samples (smooth, medium, and rough). .... 70
Figure 24	Removal of specimen slope from AIMS scanlines showing: (a) Measured heights and linear regression; (b) Normalized heights with regressed surface line at zero. .... 71
Figure 25	The relationship between lab (AIMS) and field (CT Meter) MPD values for different segment lengths: (a) Three inch (75) mm, (b) Two inch (50 mm), (c) One inch (25mm)..... 72
Figure 26	Relationship between predicted MPD (from AIMS and regression equation, for three segment lengths) and measured MPD (from CT Meter) for the three verification pavement cores..... 74
Figure 27	Average MPD values for three different texture types, based upon 50 mm (2 inch) segment lengths..... 75
Figure 28	Relationship between mean RMS from AIMS and field (CT Meter) MPD. .... 77
Figure 29	Mean AIMS RMS values by direction of scanline. .... 77

**LIST OF TABLES**

	Page
Table 1	Materials tested, indicating PG and SPG grades (N=nitrogen). ..... 17
Table 2	Strain sweep test results for stirred can recovery residues ..... 28
Table 3	Strawman emulsion residue specification ..... 31
Table 4	Linear regression equations of sand patch MTD versus CT Meter MPD from various sources, including the regression equation developed from data in this project..... 52



## 1. THESIS INTRODUCTION

This thesis project explored two aspects of the use of chip seals as a pavement preservation technique: recovery, testing, and characterization of emulsion residue (the chip seal binder); and characterization of pre-existing pavement macrotexture, which is needed for adjustment of the emulsion spray application rate. The research conducted for this thesis was performed as a subcontract to National Cooperative Highway Research Program (NCHRP) Project 14-17, *Manual for Emulsion-Based Chip Seals for Pavement Preservation (1)*.

This section presents an introduction and describes the organization and content of the thesis.

### PAVEMENT PRESERVATION

Throughout United States history, economic development has followed the development of the transportation system and the movement of people and goods with new transportation modes replacing old ones. The United States now has the most developed transportation system in the world. With this extensive and efficient transportation system in place, focus has shifted from building new transportation systems to maintaining, preserving, expanding, and improving what is already in place.

Extending the life of existing pavements is very cost effective compared to allowing their natural deterioration which requires subsequent overlay or replacement. Hence there is currently great interest in maintaining and rehabilitating the country's roadway infrastructure. Pavement preservation represents a proactive approach to maintaining the country's existing roads and highways; and it enables state transportation agencies, which bear responsibility for the majority of the roadway system, to reduce costly, time consuming rehabilitation and reconstruction projects and the associated traffic disruptions (2).

---

This thesis follows the style of the *Transportation Research Record: Journal of the Transportation Research Board*.

## **CHIP SEALS AS A PRESERVATION TREATMENT**

Chip seals (also known in Texas as seal coats) are a pavement preservation surface treatment that is commonly used as a method for maintaining and extending the lives of asphalt concrete pavements. Chip sealing involves spraying asphalt binder or emulsion onto the surface of an existing pavement followed by application of a cover aggregate. A chip seal protects a pavement by preventing oxidation of the underlying asphalt concrete and by reducing water penetration into the underlying pavement layers. A chip seal improves a pavement by creating a skid-resistant surface and by protecting the underlying pavement from tire damage. The chip seals studied for this thesis were constructed using emulsified asphalt binders (emulsion) and natural mineral aggregate chips (1). In an emulsion, the asphalt cement is emulsified (i.e., fine droplets of asphalt are suspended in water using a surfactant) to allow it to be applied by spraying without the addition of high heat. The cover aggregate in a chip seal is commonly either naturally occurring gravel or crushed aggregate such as granite, quartzite, or trap rock (basalt). Chip seals can be applied in one or in several layers.

## **NEED FOR A NATIONAL CHIP SEAL MANUAL**

In the United States, numerous states use chip seals for pavement preservation and therefore have experience with design and construction of chip seals. Several states have written chip seal manuals (3, 4, 5). However, the best chip seal practices have not recently been consolidated at the national level. Also, many of the best chip seal practices have been developed as an “art” requiring years of experience to master rather than as engineering practice which can be standardized, quantified, and written into a manual.

The objectives of NCHRP Project 14-17 were to assess current chip seal practices utilized by the states and by other countries, and to write a national chip seal

manual for the United States on the best chip seal engineering practices for use in design and construction (*1*).

## **THESIS OVERVIEW**

Research for this thesis project included completion of the following subtasks as part of NCHRP Project 14-17 at Texas A&M University (TAMU):

### Task A

- recovery of emulsion residue (the chip seal binder) from emulsified asphalt binders used for chip seals
- testing, characterization, and grading of the emulsion residue (the chip seal binder) for performance in chip seals
- recommendation of a strawman specification for emulsion residue used in chip seals

### Task B

- measurement and evaluation of existing roadway macrotexture prior to chip seal construction projects
- recommendation of a pavement macrotexture measurement technique for use on chip seal construction projects

Recommendations from this thesis were made for inclusion in the Chip Seal Manual which was the final product required from NCHRP Project 14-17 (*1*).

## **THESIS OUTLINE**

This thesis combines two papers and several additional sections. The thesis is organized into six sections as subsequently described. Each section is related to one of the specific tasks (Tasks A and B) described previously.

Section 1 presents an introduction that includes an overview and the thesis outline.

Section 2 describes the performance graded (PG) asphalt grading system and the associated laboratory tests which were developed in the Strategic Highway Research Program (SHRP) to characterize asphalt binder for performance in hot mix asphalt concrete (HMAC) pavements (6).

Section 3 is comprised of a paper concerning the testing and grading of emulsion residues for use in chip seals using both the PG specification developed in SHRP and the surface performance graded (SPG) specification previously developed at Texas A&M University (TAMU). This corresponds to Task A of this project. The paper was published in the 2010 *Transportation Research Record* (7). The authors of the paper are Denise Hoyt, Amy Epps Martin, and Scott Shuler. Recommendations for adjustment of the SPG specification for climates included in this project are presented.

Section 4 presents a discussion and evaluation of three pavement texture measurement techniques for measuring the macrotexture of existing pavements before a chip seal is applied. This is a part of Task B of this project. Parts of this section were previously published in the final report and in the final product from NCHRP Project 14-17, the *Manual for Emulsion-Based Chip Seals for Pavement Preservation* (1). In addition, this section discusses other potential macrotexture measurement techniques and developments which were not utilized in this project.

Section 5 is comprised of a paper concerning the use of a photographic image processing technique performed in the laboratory to develop pavement surface profiles for evaluating macrotexture of pavements. The paper was published in the 2011 *Transportation Research Record* (8). The authors of the paper are Arash Rezaei, Denise Hoyt, and Amy Epps Martin. While the use of pavement cores to evaluate pavement macrotexture for chip seals is not practical, the development of a portable system using similar technology might be useful in chip seal construction.

Section 6 summarizes the conclusions and recommendations that were developed based on completion of both tasks of this project.

## **2. ASPHALT BINDER CHARACTERIZATION AND THE PERFORMANCE GRADED (PG) ASPHALT BINDER SPECIFICATION SYSTEM**

Asphalt is a chemically complex material which exhibits complex material behavior, making it difficult to predict its behavior under various loading and environmental conditions. Also, asphalts that come from different sources have different chemistries and vary from each other in their material properties and behaviors. In addition, many asphalts that are used as pavement binders have polymers or rubber added to them to improve their properties as paving materials; this also adds complexity to their behavior. In order to classify or grade asphalts for use as pavement binders, their material behavior must be characterized and the material parameters which correlate to their performance as pavement materials must be understood.

Asphalts are thermoplastic and viscoelastic materials. The thermoplastic nature causes an asphalt to soften when heated and to harden when cooled. In addition, an asphalt is viscoelastic within a certain temperature range, meaning that it exhibits the mechanical properties of both viscous flow and elastic deformation (9). Because of its viscoelastic nature, asphalt behavior depends on rate of loading. The effects of time and temperature are related for this thermo-rheologically simple material: the behavior of asphalt at a high temperature is equivalent to that over a long time of loading; and the behavior at a lower temperature is equivalent to that over a shorter time of loading. This is known as the time-temperature superposition concept (6).

This section discusses asphalt binder behavior, the parameters used to describe that behavior, and the testing and grading methods for classifying asphalt binder.

## **HIGH TEMPERATURE BEHAVIOR**

In hot temperatures (e.g. in a desert climate or in hot sunny summer weather) or under sustained loads (e.g. under slowly moving or parked trucks), asphalt binder softens and behaves like a viscous liquid in which the aggregate structure helps to support the traffic loads. At temperatures above 60°C (140° F), asphalt binder is assumed to act like a Newtonian fluid with a constant viscosity that does not depend on the rate of shear strain ( $\dot{\epsilon}$ ).

## **LOW TEMPERATURE BEHAVIOR**

At cold temperatures (e.g. on winter days) or under rapidly moving loads (e.g. under fast-moving trucks), asphalt binder acts like an elastic solid. Elastic solids deform when loaded and return to their original shape when unloaded. Asphalt binder can become too brittle and crack under repeated loading (fatigue) or extreme cold temperatures (thermal cracking) ( $\dot{\epsilon}$ ).

## **INTERMEDIATE TEMPERATURE BEHAVIOR**

Environmental conditions often lie between extreme hot and cold temperatures. In intermediate temperature conditions, asphalt binder behaves both like a viscous liquid and an elastic solid. Also at moderate temperatures, asphalt binder becomes a shear thinning liquid in which the viscosity decreases as the rate of shear strain increases. These characteristics make it a complex material ( $\dot{\epsilon}$ ).

## **RHEOLOGY**

Rheology is the science of the deformation of solids and the flow of liquids under applied stresses or strains. Flow and deformation are expressed in terms of the material's

elastic, viscoelastic, and viscous properties. Parameters which measure the material properties of asphalt binders are needed to describe and quantify their rheological behavior, and these parameters can be used to provide the basis for a performance-based asphalt binder specification. The basic rheological parameters currently used to characterize the behavior of asphalt binders include the following (10, 11):

$G'$ , the elastic (or storage) modulus of the asphalt binder, which represents energy stored in the binder during repeated loading cycles;

$G''$ , the viscous (or loss) modulus of the asphalt binder, which represents energy lost in permanent deformation of the binder during repeated loading cycles;

$G^*$ , the complex modulus, which characterizes the total amount of energy used to deform the asphalt binder (or the total resistance of the material to deformation under load), and includes both the elastic and the viscous components;

$\delta$ , the phase angle, which describes the relative distribution between the elastic part and the viscous part of the asphalt binder's resistance to deformation. The phase angle is the difference between the phase of the sinusoidally varying input (the applied stress) and the phase of the output (the resulting strain), which also varies sinusoidally at the same frequency.

When the stress-strain behavior of the asphalt binder is completely elastic, the applied stress and the resulting strain are in phase and the phase angle is  $0^\circ$ . When the asphalt binder's response is completely viscous, the resulting strain is  $90^\circ$  out of phase with the applied stress and the phase angle is  $90^\circ$ .

The rheological properties of asphalt binder vary with temperature in a non-linear fashion below  $60^\circ\text{C}$  ( $140^\circ\text{F}$ ), and therefore measurements above  $60^\circ\text{C}$  ( $140^\circ\text{F}$ ) cannot be extrapolated adequately to describe the asphalt binder properties at lower temperatures. Consequently, in order to specify the rheological properties below  $60^\circ\text{C}$  ( $140^\circ\text{F}$ ), it is important that the asphalt binder properties be measured in this temperature range (12).

## **ASPHALT BINDER GRADING**

As the asphalt paving industry developed, it became evident that the uncertainties in asphalt binder material requirements needed to be minimized. Standardized methods were needed to determine fundamental properties, especially the consistency (or viscosity) of the asphalt binders obtained from different sources (13) and those modified with different additives. Several grading systems had been previously developed by the asphalt binder industry and used to describe paving asphalt binders, but these had used simplistic and sometimes empirical index testing to grade the asphalt binders. A different kind of a grading scheme for paving asphalt binders was needed.

## **PG GRADING FOR ASPHALT BINDERS**

During the Strategic Highway Research Program (SHRP) in the 1980s and 1990s, asphalt binder test protocols and equipment were developed which were relatively blind to asphalt binder composition. These tests were developed with the intention of being suitable for both unmodified and modified asphalt binders from different sources, and they focused on measuring specification properties at critical pavement design temperatures (11, 12). The SHRP researchers developed new testing equipment to measure viscoelastic asphalt binder properties at in-service temperatures that are related in a rational way to pavement performance. Pavement performance in HMAC is defined in terms of resistance to the three primary forms of distress: rutting, fatigue cracking, and low temperature cracking (6, 11, 14).

The Superpave<sup>TM</sup> (Superior Performing Asphalt Pavements) system was developed, including the performance graded (PG) specification for grading asphalt binders. This system is capable of discriminating between asphalt binders obtained from different sources and between asphalt binders modified with different polymers. In addition, the SHRP Superpave<sup>TM</sup> PG specification accomplished several other important advances over the previous simpler grading methods. It incorporated use of the Pressure



Aging Vessel (PAV) to simulate long-term aging of the asphalt binder in the field; and it characterized asphalt binders at low temperatures. It also allowed for selecting a level of reliability in the asphalt binder selection processes. The asphalt paving industry regarded these advances as significant progress in asphalt binder characterization. (14).

The PG system measures complex shear modulus ( $G^*$ ) and phase angle ( $\delta$ ) of asphalt binder using the dynamic shear rheometer (DSR) for hot and intermediate temperatures. It measures the stiffness ( $S(t)$ ) and the rate of change of the stiffness ( $m$ ) of asphalt binder using the bending beam rheometer (BBR) for cold temperatures (6).

## DSR

The DSR is an oscillatory shear test used to estimate the potential of an asphalt binder for undergoing viscous deformation at high temperatures that leads to permanent deformation, and for undergoing viscoelastic deformation at intermediate temperatures that leads to permanent deformation and fatigue cracking (12). The DSR equipment used in this project was a Malvern-Bohlin DSR II system and is shown in Figure 1.

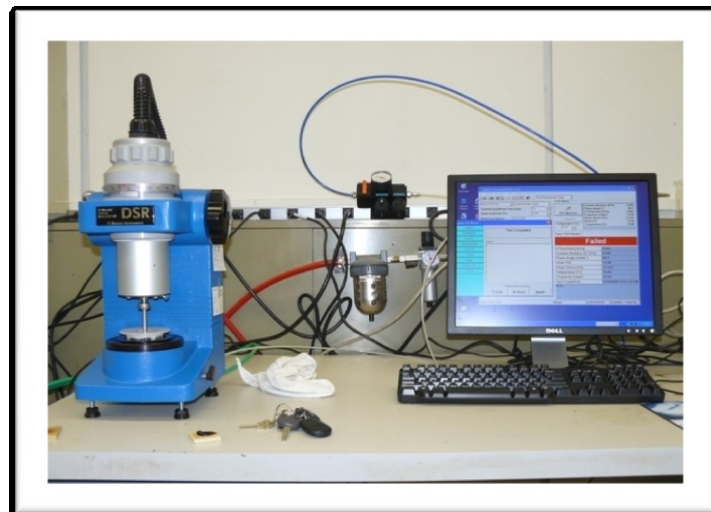


**FIGURE 1** Dynamic shear rheometer (DSR) equipment at McNew Laboratory, Texas A&M University. DSR is at the left, and computer screen is at the right. A sample in a mold can be seen on the table in front of the DSR.

In the DSR, asphalt binder is sandwiched between two parallel plates which are rotated in a sinusoidal manner with respect to each other; and the sandwiched asphalt binder is thus subjected to an alternating stress and strain. The ratio between stress and strain is calculated as follows and is called the complex shear modulus,  $G^*(\omega)$ :

$$G^*(\omega) = (\tau_{\max} - \tau_{\min}) / (\gamma_{\max} - \gamma_{\min}) \quad (1)$$

The complex shear modulus is a time dependent parameter, and its magnitude depends on the test frequency,  $\omega$ . Since the shear stress  $\tau$  and the shear strain  $\gamma$  vary sinusoidally with time, the absolute or 'peak to peak' values (determined as the maximum minus the minimum stress and strain values) are used in calculating the complex modulus (12).

The phase angle is calculated as the difference between the phase of the sinusoidally varying applied stress and that of the resulting strain, which also varies sinusoidally at the same frequency.

## **BBR**

The BBR is a beam-loading creep test used to characterize the low temperature properties of the asphalt binder in order to predict susceptibility to thermal cracking at low temperatures (12). The BBR equipment used in this research is shown in Figure 2.

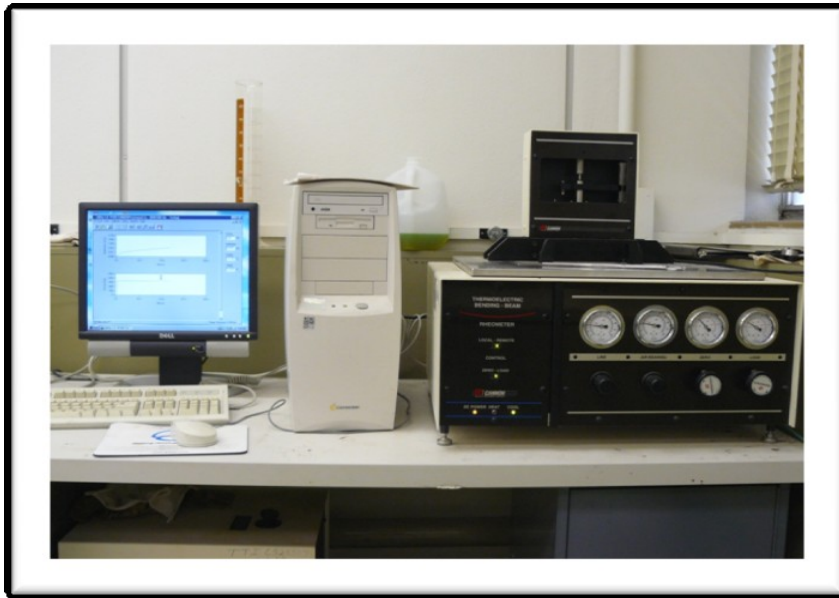


**FIGURE 2 Bending beam rheometer (BBR) and computer equipment at McNew Laboratory, Texas A&M University.**

The BBR applies a constant load for a period of time to the center of a simply supported asphalt binder beam. The asphalt binder beam is 127 mm (5.00 inches) long, 12.7 mm (0.500 inch) wide, and 6.3 mm (0.248 inch) thick, and is supported at the ends on metal supports that are 100 mm (3.94 inches) apart. During loading, the deflection of the center of the beam is continuously measured; and the time history of load and deflection are generated (10). Beam theory is used to calculate the creep stiffness,  $S(t)$ , and the rate of change of creep stiffness,  $m$ -value. The equation for obtaining the creep stiffness,  $S(t)$ , is:

$$S(t) = \frac{PL^3}{4bh^3} \delta(t) \quad (2)$$

where  $S(t)$  = creep stiffness at time  $t$  ( $\text{N}/\text{mm}^2$ );

$t$  = time of testing (seconds);

$P$  = constant applied load (N);

$L$  = distance between supports, 102 mm

b = beam width, 12.5 mm

h = beam thickness, 6.25 mm

$\delta(t)$  = deflection (mm) at time t

The desired value of the creep stiffness at minimum pavement design temperature occurs when the asphalt binder beam has been loaded for 2 hours to simulate changes in temperature in the field. However, SHRP researchers determined that, using the concept of time-temperature superposition, an equal creep stiffness can be obtained by increasing the test temperature by 10° C (50° F) for a shorter 60 second loading time. This shortened test duration and warmer temperature make the test easier to perform.

The m-value of the BBR test is the rate of change of the creep stiffness with time, and is calculated as the slope of the log of stiffness versus log of time curve. The m-value at 60 seconds is the critical value for the PG specification (6).

### **SPG GRADING FOR CHIP SEAL EMULSIONS**

The surface performance graded (SPG) specification was developed at Texas A&M University (TAMU) for grading asphalt binders used in surface treatments. It was based on the PG specification developed by SHRP for HMAC binders (14, 15), but modified to account for differences in critical distress, aging conditions, and appropriate temperatures as compared to conventional HMAC. The SPG specification assumes that appropriate design and construction practices have been followed, and it considers asphalt binder properties after construction. The SPG system is primarily based on temperature grading criteria to preclude aggregate loss and bleeding, which are the predominant surface treatment distresses resulting from inappropriate material selection (15). The final SPG specification includes suggested limiting values for design parameters for high and low pavement surface design temperatures (14).

### **3. SURFACE PERFORMANCE-GRADING SYSTEM TO GRADE CHIP SEAL EMULSION RESIDUES<sup>1</sup>**

#### **INTRODUCTION**

In the current age of pavement preservation and preventive maintenance, the adequate performance of pavement surface treatments is vital; and improved methods of design and construction are needed. An important part of asphalt surface treatment design is selection of an appropriate binder type and grade.

Binder grading systems have progressed from early empirically based systems to systems based upon materials characterization related to performance and resistance to distress. Because asphalts are viscoelastic materials, their behavior depends upon both temperature and rate of loading. Climate and traffic therefore should be considered in grading and choosing asphalt binders for pavement construction projects.

Chip seals are a common pavement surface treatment. A recent chip seal research project utilized and compared two asphalt binder grading systems which characterize materials based on laboratory tests that take these considerations into account. These binder grading systems are performance-based and are designed to increase the likelihood of success of pavement projects, including chip seals.

#### **MOTIVATION**

The Performance Grading (PG) asphalt binder grading system as described in Superpave Series SP-1 (6) is widely used as the specification for grading and selecting asphalt binders. The PG specification was developed for use in hot mix asphalt concrete

---

<sup>1</sup> Paper presented at the 89<sup>th</sup> Annual Meeting of the Transportation Research Board, January, 2010, Washington, D.C., and published in the 2010 series of the *Transportation Research Record: Journal of the Transportation Research Board* (7). Copyright, National Academy of Sciences. Reproduced with permission of the Transportation Research Board.

(HMAC) pavement layers. However, the PG system is not applicable to classifying and choosing binders for use in pavement chip seals. Typically, chip seals are thin layers of binder and aggregate placed on the pavement surface to protect and restore the surface. Chip seals differ from full depth HMAC layers in construction methods, structural functions, behavioral responses, distress types, and environmental exposure. The Surface Performance Grading (SPG) binder grading system was created in the early 2000s to classify binders for use in chip seals (14, 16). However, the SPG system has not previously been widely accepted or utilized.

Currently there is renewed interest in the SPG system through the Emulsion Task Force (ETF) of the Federal Highway Administration's Pavement Preservation Expert Task Group (PPETG). The charge of the PPETG is "to assure the widespread adoption by SHA's [state highway agencies] of pavement preservation and preventive maintenance techniques" (17), and the PPETF is investigating the characterization of emulsions for use in surface treatments. National Cooperative Highway Research Program (NCHRP) 14-17 is a national research project which will culminate in a chip seal manual. This paper describes the binder characterization and grading which was performed for this project, which included use of the SPG specification.

## **THE SURFACE PERFORMANCE-GRADED (SPG) SPECIFICATION**

In 2000, the Texas Department of Transportation (TxDOT) initiated a research project with Texas A&M University (TAMU) to develop a performance based grading and specification system for chip seal binders (14, 16). The surface performance-graded (SPG) specification was created. The tests used in the specification are conducted with standard PG testing equipment; and the analyses are performance-based and consistent with chip seal design, construction, behavior, in-service performance, and associated distresses (14, 16). TAMU researchers recommended that the SPG needed field validation; and in 2005, TxDOT and TAMU completed an initial field validation study in Texas (15, 18) which assessed and modified the SPG specification. The initial validation

included three visual distress surveys over a one-year performance monitoring period for 45 field sections in Texas. Predominant chip seal distresses (raveling and bleeding) associated with inappropriate material selection were monitored, and a surface condition index (SCI) was utilized with a threshold of 70 percent between adequate and inadequate performance (15, 18).

## **OBJECTIVE**

The objective of this paper is to promote the continued development and use at the national level of the SPG binder grading system for chip seals. This paper describes the use of both the PG and the SPG binder grading systems to grade and compare several base binders and recovered residues from corresponding emulsions designed for use in chip seals.

## **DESCRIPTION OF CONTENTS**

This paper describes the materials characterization task included in NCHRP 14-17. Discussions of the materials studied, the emulsion recovery methods, and the materials tests are presented. Results and analyses are offered, including statistical analyses of some of the results. Conclusions are presented with recommendations for future research.

## **EXPERIMENTAL DESIGN OF NCHRP 14-17 BINDER CHARACTERIZATION**

The standard PG system (6) and the modified SPG system (14, 16, 15, 18) were both used to grade all of the base binders and the recovered emulsion residues in this research. The climate in which a pavement is placed is the main criterion used to determine the selection of a binder grade in both of these systems. In the future, the

expected traffic level may be incorporated by an adjustment to the binder grade selection for traffic speed and loading.

## **MATERIALS**

Seven emulsions were included in this project. Five of the emulsions and their base binders were obtained from the supplier (emulsions 1-5). Field projects were not included in this research for the first five emulsions; they were used for laboratory study only. The other two emulsions were obtained from field chip seal projects selected from different environments (emulsions 6-7): one in the high desert of Arches National Park in Utah, and one on a county road along the Rocky Mountain front range in Frederick, Colorado. Table 1 indicates the types of the emulsions and, when known, the PG grades of the base binders as reported by the supplier.

## **EMULSION RECOVERY METHODS**

Two emulsion residue recovery methods were used in NCHRP 14-17 to extract the water from the emulsions and to supply de-watered bitumen residue for the material properties testing. The residue recovery methods employed were:

- Hot oven (with nitrogen blanket)
- Stirred can (with nitrogen purge)

The hot oven method is similar to the recovery method described in ASTM D244-97C (19) with the modification that nitrogen flows over the sample to prevent oxidation and consequent aging of the material. A beaker containing 50 g of emulsion is placed in a 163°C oven with nitrogen flowing over it. After 2 hours in the oven, the emulsion is stirred with a glass rod and then remains in the oven for 1 hour more. The residue, about 30 g from each beaker, is then stored in an ointment tin until testing.



**TABLE 1 Materials tested, indicating PG and SPG grades (N=nitrogen).**

Emulsion	Emulsion Type	Expected Base Grade	Recovery Method	PG Grade from Tests	Continuous PG Grade	SPG Grade from Tests	Continuous SPG Grade
1	RS-2P	PG 64 -28	Base Asphalt	PG 64 -34	67.8 -34.2	SPG 70 -24	71.7 -24.0
			Stirred Can with N	PG 64 -34	69.3 -34.1	SPG 73 -18	73.0 -21.3
			Hot Oven-N Blanket	PG 64 -34	69.5 -34.1	SPG 73 -18	73.4 -21.1
2	CRS-2	na	Base Asphalt	PG 58 -28	60.2 -30.7	SPG 61 -18	63.1 -19.4
			Stirred Can with N	PG 58 -28	62.9 -31.0	SPG 64 -18	66.4 -19.2
			Hot Oven-N Blanket	PG 58 -28	61.9 -32.1	SPG 64 -18	64.5 -20.7
3	RS-2	PG 64 -22	Base Asphalt	PG 64 -22	66.9 -27.1	SPG 67 -12	69.7 -14.7
			Stirred Can with N	PG 64 -22	68.2 -26.8	SPG 70 -12	71.4 -15.9
			Hot Oven-N Blanket	PG 64 -22	68.5 -26.5	SPG 70 -12	71.7 -15.1
4	CRS-2P	PG 64 -28	Base Asphalt	PG 64 -28	67.6 -32.9	SPG 70 -18	70.8 -22.2
			Stirred Can with N	PG 64 -28	68.6 -33.2	SPG 70 -18	72.3 -22.9
			Hot Oven-N Blanket	PG 64 -28	69.2 -33.7	SPG 70 -18	72.9 -23.4
5	HFRS-2P	PG 70 -28	Base Asphalt	PG 58 -28	62.3 -30.4	SPG 64 -18	65.7 -18.7
			Stirred Can with N	PG 58 -28	63.4 -31.6	SPG 67 -18	67.0 -20.1
			Hot Oven-N Blanket	PG 58 -28	63.3 -31.8	SPG 64 -18	66.9 -20.0
6-UT	LM CRS-2	na	Stirred Can with N	PG 70 -22	74.7 -26.4	SPG 76 -12	78.7 -15.3
			Hot Oven-N Blanket	PG 76 -22	76.7 -26.3	SPG 79 -12	80.9 -15.7
7-CO	HFRS-2P	na	Stirred Can with N	PG 70 -28	72.0 -32.0	SPG 76 -18	76.6 -21.1
			Hot Oven-N Blanket	PG 70 -28	72.7 -31.6	SPG 76 -18	77.0 -20.3
8-WA	CRS-2P	PG 64 -22	Stirred Can with N	PG 64 -28	64.1 -28.0	SPG 67 -18	67.6 -18
			Hot Oven-N Blanket	PG 64 -22	64.0 -27.9	SPG 67 -12	67.1 -17.1

For the stirred can method, a gallon can containing 1250 to 1300 g of emulsion is wrapped in heating tape and placed over a burner<sup>2</sup>. The emulsion is stirred constantly with an impeller blade while being heated at 163°C for 170 minutes. Nitrogen is bubbled up through the can and also flows over the top of the material to prevent oxidation and consequent aging of the material. After 170 minutes, the can is removed from the heat source and covered. The residue, about 800 g, is stored in the gallon can until testing.

A third residue recovery method known as the low temperature evaporative technique (20) is currently being recommended by other researchers (21, 22) to preclude destruction of the polymer matrix during residue recovery. This project conducted a preliminary comparison of the residue recovery methods used in this study with the low temperature evaporative method, and the findings have been presented elsewhere (23).

## LABORATORY TESTS

### Rheology Tests

The binder characterization tests utilized the same equipment and some of the same tests as specified in the PG system (6), but with different limiting criteria. For each test, two replicate specimens were tested.

The dynamic shear rheometer (DSR) was used to measure the rheological properties of the binders, complex shear modulus  $G^*$  and phase angle  $\delta$  in the form ( $G^*/\sin \delta$ ), at high temperatures. Unaged binder was tested at the high temperatures, which is the critical condition for early strength development in chip seals.

All of the binders in this project were aged using only the pressure aging vessel (PAV), as described in the PG specification (6). Rolling thin film oven (RTFO) aging was omitted as RTFO is not applicable to emulsions because they are not heated to high temperatures during emulsification and construction.

---

<sup>2</sup> Correction: For the stirred can residue recovery method, the gallon can containing the emulsion is wrapped in insulation and placed on heating tape. Heating tape provides more even heating to the outside of the can than a burner produces.

The bending beam rheometer (BBR) was used to measure bending properties of the binders (stiffness,  $S$ , and rate of change in binder stiffness with time,  $m$ -value) at cold temperatures. PAV aged binder was used in the BBR to simulate long-term in-service aging that may cause failure at cold temperatures for chip seals. PAV aging simulates approximately the first hot and cold seasons of a chip seal which is when most chip seal failures occur (14, 16).

The DSR was also used to measure the properties  $G^*$  and  $\delta$  in the form ( $G^* \sin \delta$ ) which is related to fatigue in HMAC at intermediate temperatures on PAV aged material. The ( $G^* \sin \delta$ ) parameter was used to check that the materials met the intermediate temperature criteria for the PG grade as determined from the high and low temperature testing.

Strain sweeps were also performed using the DSR at 25° C on both unaged and PAV aged material. The critical performance parameters for a chip seal during its first year are resistance to raveling and aggregate loss at both high and low temperatures. Strain sweep testing of emulsion residue in the DSR is currently being investigated elsewhere (22, 24) to assess whether an emulsion residue develops adequate strain tolerance and stiffness to prevent the bond between aggregate and emulsion residue from failing.

### **Strain Sweep Tests**

Strain sweeps and their correlation with the sweep test, ASTM D-7000 (25), have been investigated elsewhere (24) for evaluating the potential of emulsions to resist raveling during curing after chip seal construction. Strain sweep testing was investigated in this study as an addition to the SPG system for evaluating strain tolerance and resistance to raveling of emulsion residues during curing and at early ages.

The strain sweeps were conducted using the DSR at 25° C (8 mm plates, 2 mm gap) on both unaged and PAV aged material to show the reduction in  $G^*$  with increasing strain. Strain sweep test results are affected by how the testing is performed and by the

parameters input into the DSR. The DSR is continually oscillating during strain sweep testing. Input to the DSR requested strains of 1 to 50%, and the strain sweeps were initiated at 1%. A thermal equilibrium time of 10 minutes after mounting the sample and before testing started was used, with an angular loading frequency of 10 radians/second and a linear loading sequence with time. A delay time of 1 second after the load (strain) was incremented but before the measurements were taken was chosen, and between 20 and 30 strain increments were imposed and measured during each test. Using these parameters resulted in a test time for each strain sweep of approximately 1 to 2 minutes (after thermal equilibrium).

### **Chemical Tests**

Several additional tests were performed to assess characteristics that were not included in the rheological or strain sweep testing.

Gel permeation chromatography (GPC) was performed on each recovered residue to determine that all of the water had been removed during the residue recovery process. GPC is a size exclusion chromatography (SEC) method of molecular analysis. Presence or absence of a peak at a time of 35 to 37.5 minutes on the GPC chromatogram indicates the presence or absence of water in the residue.

Fourier transform infrared (FT-IR) spectroscopy was performed on the residues from the five laboratory emulsions to obtain an indication of whether the recovery methods caused oxidation of the materials. The emulsions from the 3 field projects were not included in the spectroscopy testing. The infrared spectra were plotted, and then the area under the wavenumber band from 1820 to 1650  $\text{cm}^{-1}$  was integrated to determine the carbonyl area. The integrated carbonyl area can be used to represent the extent of oxidation in the materials (14, 23, 26). This can be compared for the base asphalt versus the recovered residues to determine if the emulsifying and residue recovery processes caused oxidation. It can also be compared among different residue recovery methods to determine if one recovery method causes more oxidation than another.

## BINDER GRADING

Emulsion residues from the two recovery procedures and some of their base asphalts were graded according to the PG system developed for HMAC (6) and the SPG system developed for surface treatments (14, 16, 15, 18) but both without RTFO aging. As compared to the PG system, the SPG system incorporates the following modifications:

- high temperature DSR tests are performed at 3° increments, allowing material performance to be discriminated over a finer scale of temperature;
- the high temperature design condition for the SPG system is specified as the pavement surface temperature;
- DSR testing at high temperatures on unaged binders is expected to reflect the critical condition for early-age surface treatments; and a threshold value of 0.650 kPa minimum is used as the limiting value for  $(G^*/\sin \delta)$  for SPG high temperature grading, as recommended by TAMU (15, 18);
- DSR testing at intermediate temperature(s) in the SPG system is not performed because previous research (14, 16) found that the intermediate temperature test results did not discriminate between binders that performed well and those that did not;
- DSR strain sweep testing at an intermediate temperature of 25° C was instead performed for a revised SPG system to assess strain susceptibility and resistance to raveling of the emulsion residues, especially during the critical first season after construction;
- BBR testing at low temperatures is expected to reflect the critical condition for raveling caused by traffic loading on stiff materials; therefore, low temperature properties based on BBR testing were determined at the fastest possible loading time, 8 seconds, and the actual test temperature was used;
- threshold values used for BBR tests at 8 seconds were 500 MPa maximum for SPG flexural stiffness and 0.240 minimum for SPG m-value;

- the SPG criteria used were developed using Texas chip seal projects (14, 16). These criteria should be developed or verified for other states or regions in the future.

## **RESULTS AND ANALYSES**

### **DSR Results: High Temperatures**

For the high temperature characterization in both grading systems, plots were generated of  $(G^*/\sin \delta)$  versus temperature. At the high temperatures, the base binders in every case exhibited lower test parameters  $(G^*/\sin \delta)$  than did the recovered residues. This is possibly due to stiffening and aging of the residues during either the emulsification process or the residue recovery process.

### **BBR Results: Low Temperatures**

For the low temperature characterization in both grading systems, plots were generated of  $S$  versus temperature and of  $m$ -value versus temperature. The plots from the BBR test results indicated that the base binders and the recovered emulsion residues had similar cold temperature properties. Aging of the materials (and possibly exposure to cold temperatures) seemed to affect the base asphalts and the recovered residues so that they exhibited similar properties at cold temperature after PAV aging. This result may indicate that, after PAV aging and consequent oxidation, the polymers and additives no longer had an effect on the stiffness properties.

### **DSR Results: Intermediate Temperatures**

All of the materials passed the PG criterion for  $(G^*\sin \delta)$  at the specified intermediate temperatures. All of the materials also passed for at least one additional

(i.e. colder) temperature. Intermediate single-temperature DSR tests were not performed for the SPG grading; but strain sweeps were performed at 25° C to evaluate strain sensitivity at an average ambient construction temperature.

### **PG and SPG Grading**

Both PG and SPG grades were determined for all of the base binders and recovered residues, and the results are shown in Table 1 (above). Interpolation was used to determine the continuous grades. The continuous grades can be used to discriminate more accurately the differences in grading among the different recovery methods for the same emulsion residue.

In general, the PG grades were consistent for the base binder and the residues from both recovery methods, as were the SPG grades. However, examination of the continuous grades indicated that the base binder grades were slightly different from the grades of the recovered residues.

Use of the SPG system resulted in a higher continuous grade at both the high and the low temperature ends than the continuous grade with the PG system. The average difference in the high temperature continuous grades (SPG minus PG) was +3.6° C. The average difference in the low temperature continuous grades (SPG minus PG) was +11.3° C. This large difference is due in part to the lack of a time-temperature shift in the SPG grading due to the differences in low temperature distress addressed by the specification (raveling under traffic loading in SPG versus low temperature cracking caused by slow changes in temperature for PG).

### **Chemical Analysis Results**

The GPC chromatograms from all of the residues from both of the recovery processes indicated that water was absent from the recovered emulsion residues and had therefore been completely removed from the emulsions during the recovery procedures.

The carbonyl areas calculated from FT-IR spectra for the five laboratory emulsions indicated that the recovered binders were all slightly more oxidized than the base binders. This oxidation could have occurred during emulsification or during the residue recovery process.

### **Statistical Analyses Summary**

The rheological data collected with the DSR and the BBR were analyzed statistically using Analysis of Variance (ANOVA) and Tukey's Honestly Significant Differences (HSD) multiple comparison techniques. A level of confidence of  $\alpha = 0.05$  was used in all of the analyses. The objective was to determine if there were statistical differences between the emulsions and between the recovery methods.

When comparing the DSR data by recovery method, the analysis results statistically grouped the recovery methods of stirred can and hot oven together, and the base binder ("no recovery") was grouped separately for the emulsions with base binders available (1-5). Both recovered residues were stiffer, with larger values of  $\log(G^*/\sin \delta)$ , than the base binders, but not stiff enough to change the high-temperature PG grade for emulsions 1-5. With smaller temperature increments, the high-temperature SPG grade did change to a larger value for four of emulsions 1-5.

The recurring result from all of the analyses of the BBR measurements was that the recovery method (with base binders included as "no recovery") did not practically affect the response variables S or m-value for any of the recovered residues. This result seemed to indicate that, after PAV aging and consequent oxidation, the polymers and additives no longer had an effect on the stiffness properties.

The spectroscopic data were also analyzed statistically using Analysis of Variance (ANOVA) and Tukey's Honestly Significant Differences (HSD) multiple comparison techniques. A level of confidence of  $\alpha = 0.05$  was used in all of the analyses. Statistical analyses of carbonyl areas indicated that aging due to the two recovery methods used in this experiment did not differentiate the recovery methods from each



other. The base binders and the recovered residues were statistically different, but the two recovery methods were similar to each other in terms of oxidative effects.

### **Strain Sweep Results**

Strain sweeps were conducted in this research on unaged and PAV aged materials. The unaged material represented the binder residue after the chip seal was constructed and the binder had cured with complete water removal. The PAV aged material represented the binder residue after the chip seal would have been in place for approximately one summer (high temperature) and one winter (low temperature). The majority of chip seal failures occur during either the first summer or the first winter (14).

Comparison of the plots of  $G^*$  versus % strain indicate that the magnitudes of the  $G^*$  and strain values and the shapes and rates of change of the curves are significant for comparing materials and characterizing strain tolerance. For comparison, the strain sweep curves from the stirred can recovery residues for aged and unaged materials in this project are shown in Figure 3.

Materials with high strain tolerance exhibit slow deterioration of  $G^*$  with increasing strain level, indicating that the material maintains stiffness and holds together under repeated and increasing loads. Emulsions 1, 2, 4, and 5 in an unaged state in Figure 3 exhibited this behavior. These materials were sticky, stretchy, and stringy to handle in the laboratory, even after strain sweep testing. Materials with less strain tolerance have curves that quickly develop steeper downward slopes, indicating that the material loses stiffness with increasing strain. Emulsions 2, 3 and Utah Arches in a PAV aged state in Figure 3 are examples of this type of behavior. These materials were very stiff and broke off of the test plates in a brittle manner after the strain sweep testing was completed. The slopes of the curves were steeper for the PAV aged materials than for the unaged materials, as can be seen by comparing the Utah Arches unaged and the Colorado Frederick PAV aged curves in Figure 3. This relationship can also be seen by

looking at the curve for emulsion residue 3 unaged versus those for emulsion residues 4 and 5 PAV aged.

During early curing, the binder material must develop enough stiffness to be able to carry vehicle loads before the chip seal is opened to traffic. A minimum level of  $G^*$  must be attained at which an emulsion has cured enough and lost enough water for emulsion residue to support traffic. Emulsion curing after chip seal construction is commonly used in the field to determine when a chip seal can be opened to traffic. This could be correlated with the initial  $G^*$ , or  $G_i^*$ , from the strain sweep testing to determine a minimum  $G^*$  for traffic bearing capacity.

Researchers at the University of Wisconsin have conducted testing on binders during curing and have recommended the following criteria for determining strain tolerance and failure of the emulsion residue during curing (22):

- a) 10% reduction in  $G^*$ , or  $0.10G_i^*$ , which characterizes strain tolerance and indicates that the material is behaving nonlinearly and is accumulating damage;
- b) 50% reduction in  $G^*$ , or  $0.50G_i^*$ , which defines failure of the material.

This study found that, the more stiff the emulsion residue initially is and the more cured and then aged it becomes, the more difficult it is to reach 50%  $G_i^*$  and even 90%  $G_i^*$  in strain sweep testing. This is especially true for PAV aged materials. The maximum stress that the Malvern-Bohlin DSR II can induce is 99,470 Pa. None of the materials in this study reached 50% of  $G_i^*$  using the test parameters described previously. Most of the unaged and only a few of the PAV aged materials reached 80%  $G_i^*$ , as shown in Table 2. It is possible that intermediate reductions in  $G_i^*$  might be used so that the behavior of the fully cured residues can be characterized even when 50% or 90%  $G_i^*$  cannot be attained. Another solution could be the use of different test parameters.

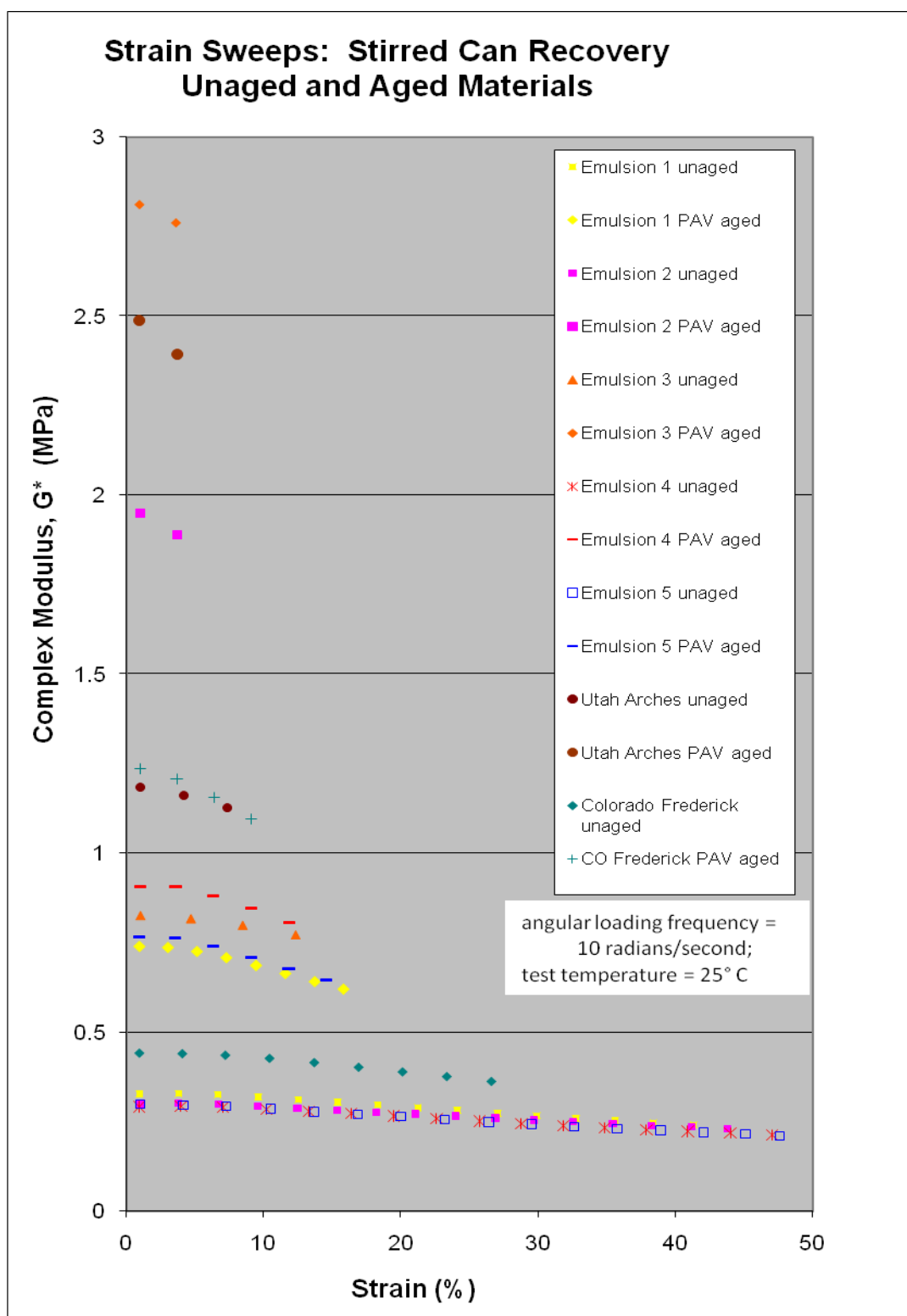


**FIGURE 3** Strain sweep results for the stirred can recovery residues.

**TABLE 2 Strain sweep test results for stirred can recovery residues.**

Emulsion	Recovery	Unaged $G_i^*$ (Pa, at 1% $\gamma$ )	% $\gamma$ at $0.90G_i^*$	% $\gamma$ at $0.80G_i^*$	% $\gamma$ at $0.50G_i^*$	Aged $G_i^*$ (Pa, at 1% $\gamma$ )	% $\gamma$ at $0.98G_i^*$	% $\gamma$ at $0.90G_i^*$	% $\gamma$ at $0.80G_i^*$	% $\gamma$ at $0.50G_i^*$
1	base	241,120	21.23	34.74	n/a	987,120	4.95	10.88	12.67	n/a
1	stirred can	326,460	19.20	31.22	n/a	883,620	5.01	11.86	14.15	n/a
1	hot oven	337,500	19.79	32.67	60.06	844,030	5.53	11.46	14.82	n/a
2	base	248,290	25.72	6.18	84.03	1,448,300	3.93	7.31	8.62	n/a
2	stirred can	298,170	22.17	38.31	n/a	1,948,300	2.77	5.29	6.40	n/a
2	hot oven	318,660	21.32	36.98	63.37	1,385,600	4.33	7.68	9.01	n/a
3	base	747,630	14.84	16.71	n/a	3,329,800	2.31	n/a	n/a	n/a
3	stirred can	825,740	13.26	15.13	n/a	2,811,300	3.62	n/a	n/a	n/a
3	hot oven	813,970	13.64	15.35	n/a	3,163,400	2.14	n/a	n/a	n/a
4	base	219,060	25.41	44.14	n/a	954,040	5.24	10.92	13.11	n/a
4	stirred can	289,860	20.77	34.51	n/a	905,480	5.58	11.27	13.82	n/a
4	hot oven	257,750	24.35	34.26	n/a	778,100	4.84	11.11	16.10	n/a
5	base	266,850	22.03	38.45	n/a	1,260,200	4.92	8.81	9.91	n/a
5	stirred can	297,360	17.79	31.46	67.95	765,620	5.18	10.76	16.35	n/a
5	hot oven	286,680	17.27	30.57	70.53	801,740	3.96	10.38	15.54	n/a
6 – UT	stirred can	1,182,300	9.18	10.56	n/a	2,486,600	2.45	4.46	n/a	n/a
6 – UT	hot oven	1,203,200	9.21	10.37	n/a	2,886,400	3.33	3.84	n/a	n/a
7 – CO	stirred can	440,260	18.16	28.36	45.86	1,235,400	3.36	8.41	10.11	n/a
7 – CO	hot oven	444,800	17.92	28.20	45.42	1,198,900	3.06	7.51	10.36	n/a

Grey shading = after max DSR stress was reached; n/a = test didn't run that far

Besides differing in the rate at which  $G^*$  deteriorated with increasing strain, the materials differed in their original stiffness,  $G_i^*$ , and in the amounts of increase in  $G_i^*$  that occurred between the unaged state and the PAV aged state. Table 2 includes a summary of the  $G_i^*$ s. The stiffest material in the unaged state was the Utah Arches emulsion residue (emulsion 6), a latex modified rapid-setting emulsion. The stiffest material in the aged state was the emulsion 3 residue, a rapid-setting unmodified emulsion.  $G^*$  increased the most from the unaged to the aged state for the emulsion 3 residue. It was followed by the emulsion 2 residue, also a rapid-setting unmodified emulsion, and then by the Utah Arches emulsion 6 residue. Emulsion residues for 1, 4, 5, and Colorado Frederick (emulsion 7), all polymer modified emulsions, increased in  $G^*$  and exhibited aged behavior after the PAV aging, but not by as much as emulsion residues 2, 3, and Utah Arches (emulsion 6). Also, for emulsions 1, 4, and 5 the base binder increased in  $G^*$  considerably more than the recovered residues did, possibly indicating that either the emulsification process or the residue recovery process reduced the susceptibility of these materials to the PAV aging process.

Based on the results of the strain sweep testing, emulsions 1, 2, 4, 5, and Colorado Frederick (emulsion 7) would be expected to resist raveling due to their high strain tolerances. Emulsions 3 and Utah Arches (emulsion 6), which had very stiff residues even when unaged, would be expected to resist flushing and also might be able to be opened to traffic earlier; however, they became more brittle with aging and could therefore exhibit raveling with age. The Utah Arches project was located in the high desert where there is high heat and intense sun, and the road carries more traffic in the summer than in the winter. A stiff binder would resist deformation and raveling in these conditions. The high stiffness of the Utah Arches emulsion 6 residue might be beneficial in this environment.

### **Field Site Assessment After One Year**

The chip seal project at Fredrick, Colorado was assessed visually after one year and it looked very good. The site was snowplowed last winter for an estimated 48 days and there is only slight damage at the crown for approximately 1500 feet in over 3 miles. Embedment is approximately 60-75 percent as expected.

The chip seals at the other field sites were not evaluated as part of this project.

### **RECOMMENDATIONS AND CONCLUSIONS**

Surface Performance Grading (SPG) with additional tests but using the same equipment as used in the Performance Graded (PG) system is a step in the right direction for a performance graded specification for chip seal materials. A strawman emulsion residue specification based on that proposed through TxDOT research (15, 18) and modified based on the results of this experiment is shown in Table 3. The strain sweep thresholds were selected to reflect the significantly different performance of emulsion 3 and the Utah Arches emulsion 6. Based on the methods evaluated, the stirred can emulsion residue recovery method is recommended for use with this proposed specification.

**TABLE 3 Strawman emulsion residue specification.**

*This table presents only three SPG grades as an example, but the grades are unlimited and can be extended in both directions of the temperature spectrum using 3 and 6 °C increments for the high temperature and low temperature grades, respectively.	Performance Grade											
	SPG 64				SPG 67				SPG 70			
	-12	-18	-24	-30	-12	-18	-24	-30	-12	-18	-24	-30
Average 7-day Maximum Surface Pavement Design Temperature, °C	<64				<67				<70			
Minimum Surface Pavement Design Temperature, °C	>-12	>-18	>-24	>-30	>-12	>-18	>-24	>-30	>-12	>-18	>-24	>-30
Original Binder												
Dynamic Shear, AASHTO TP5 $\frac{G^*}{\sin \delta}$ , Minimum: 0.65 kPa Test Temperature @10 rad/s, °C	64				67				70			
Shear Strain Sweep % strain @ 0.8G <sub>i</sub> *, Minimum: 25 Test Temperature @10 rad/s linear loading from 1-50% strain, 1 sec delay time with measurement of 20-30 increments, °C	25				25				25			
Pressure Aging Vessel (PAV) Residue (AASHTO PP1)												
PAV Aging Temperature, °C	100				100				100			
Creep Stiffness, AASHTO TP1 S, Maximum: 500 MPa m-value, Minimum: 0.240 Test Temperature @ 8s, °C	-12	-18	-24	-30	-12	-18	-24	-30	-12	-18	-24	-30
Shear Strain Sweep G <sub>i</sub> *, Maximum: 2.5 MPa Test Temperature @10 rad/s linear loading at 1% strain and 1 sec delay time, °C	25				25				25			

The thresholds provided for the DSR and BBR parameters are based on validation with Texas field sections, and they likely need to be adjusted for different climates. The current thresholds result in grades of SPG 76-12, SPG 76-18, and SPG 67-

18 for the residues from the Utah Arches emulsion 6, the Colorado emulsion 7, and the Washington emulsion 8, respectively. The closest LTPPBIND weather stations (LTPPBIND Version 3.0/3.1) and Long Term Pavement Performance (LTPP) Pavement Temperature Models require SPG 61-12, SPG 58-24, and SPG 52-12 at 50% reliability, respectively, for adequate performance in Utah, Colorado, and Washington (27, 28). This discrepancy between the required emulsion residue grade for the selected climate and the actual grade of the material utilized illustrates that the thresholds, particularly for the low temperature BBR properties, may need adjustment if the field performance after the first critical year in Colorado is indicative.

Strain sweeps performed with the DSR on curing and unaged emulsion residues are recommended to evaluate strain resistance and stiffness development. These tests could be used to predict when emulsion based chip seals will develop enough stiffness to be opened to traffic. Strain sweeps could also be used to assess a material's resistance to raveling, both in newly constructed chip seals and after the critical first seasons of weather and aging. However, additional work is needed to choose proper test parameters and to refine the performance criteria.

Recovered emulsion residues were shown to be different from their base binders at high temperatures in the unaged state, but they were similar to their base binders at cold temperatures after aging. Recovered residues from the two recovery methods utilized were oxidized more than their base binders but at similar levels.

## **FUTURE RESEARCH**

Further field validation of the SPG specification criteria and extension of the grading criteria to regions other than Texas are needed before the specification for SPG can be approved and used on a national level.

Further performance monitoring of the three seal coat projects constructed and studied in this project is recommended.



Further evaluation of the residue recovery methods is needed to determine which most closely simulates emulsion residue in the field.

It is commonly agreed that there is a need to replace cold temperature testing using the BBR with an alternative test which measures  $G^*$  at cold temperatures directly. Research being done at University of Wisconsin Madison and at Western Research Institute (29) may produce a replacement test.

## 4. EXISTING PAVEMENT TEXTURE EVALUATION FOR USE IN CHIP SEAL EMULSION SPRAY RATE ADJUSTMENT<sup>3</sup>

### INTRODUCTION

In chip seal construction, the texture of the existing pavement surface affects the rate at which the chip seal binder (emulsion) must be applied. Existing pavement texture must be evaluated for adjustment of the application spray rate of the chip seal emulsion. A rough existing surface texture will soak up more emulsion than a smooth surface, making that part of the emulsion residue unavailable for the chip seal layer on the surface and thus providing less asphalt binder than is needed for durability. Therefore, the emulsion spray rate needs to be increased with increasing pavement surface texture. In the past, emulsion spray rate has been adjusted according to the experience of the construction personnel. This project assessed methods for quantifying pavement surface texture to be used for emulsion spray rate adjustment. Recommendations are made for additional research.

This section describes the texture experiments that were conducted and the pavement texture measurement methods that were utilized in this project.

### TEXTURE MEASUREMENT

Surface texture evaluation is a necessary part of the chip seal project. “Macrot texture is the texture type that is relevant to chip seals. Macrot texture is surface roughness that is caused by the mixture properties of an asphalt concrete surface or by the finishing/texturing method of a Portland cement concrete surface (30)” (1).

---

<sup>3</sup> Parts of this section were written by the thesis author and have been previously published in *NCHRP Report 680: Manual for Emulsion-Based Chip Seals for Pavement Preservation (1)* by the National Cooperative Highway Research Program. Even though this is the writing of the author, material that has been previously published in the manual is referenced as direct quote in the text.

“Previous work has indicated that either the sand patch test (31) or the circular texture meter (CT Meter) profile (32) can be used to effectively evaluate pavement macrotexture (33, 30, 34). Both of these measurements are easily performed in the field, but traffic control is needed during the measurements. The sand patch test has been used for texture measurement because it requires inexpensive equipment that is easy to obtain, and it provides acceptable measurements (35, 36). However, conducting the test is slow and exposes personnel to traffic, and results are influenced by wind and moisture” (1).

Measurement of the pavement surface macrotexture can be made more quickly with the CT Meter than with sand patch testing, and therefore use of the CT Meter exposes the technician to less traffic and accident risk. In addition, the CT Meter measurement is automated and does not depend upon operator skill like the sand patch test does (1). Finally, the CT Meter equipment is expensive. However, once the initial investment is made, the equipment is durable if taken care of; and the cost can be justified by the increased safety for the field technicians.

## **DESCRIPTION OF THE EXPERIMENT**

For this part of the project, existing pavement surface macrotexture was measured at chip seal projects at Utah Arches National Park, at a county road in Frederick, Colorado, and on US 101 in Washington state using the sand patch test and CT Meter measurements. Multiple measurements were made of both in-wheel path and between-wheel path texture on each chip seal construction site. In addition, three fabricated test slabs of varying texture (smooth, medium, and rough) were evaluated by the two test methods used in the field as well as by an additional macrotexture measurement method using the aggregate imaging system<sup>4</sup> (AIMS) in the laboratory. The three test slabs were

---

<sup>4</sup> The AIMS equipment was originally called the “aggregate imaging system” (40). The most recent version of the AIMS equipment is known as the “aggregate image measurement system” (58). These are different models of the same equipment, and both are referred to as AIMS. This thesis uses the older terminology, “aggregate imaging system”, throughout. The older model of AIMS was used for the work done for this section of the thesis; and the newer model of AIMS was used for the work reported in section 4 of this thesis. Differences in the scanline configuration between the old and the new AIMS systems are described in the text.

cast with self-consolidating concrete at Colorado State University and sent to Texas A&M University for use in comparing the surface texture measurement methods. The test slabs simulated a rough, a medium, and a smooth pavement surface texture (1). For the AIMS measurements, small samples were cut from each of the test slabs.

An additional device not used on this project, the Ames laser texture scanner, has been developed and tested elsewhere (37) and might also be useful for measuring pavement macrotexture prior to chip seal construction. Although not used in this project, the Ames scanner will be discussed in this section.

An additional related experiment was conducted in the laboratory comparing AIMS texture measurements on pavement cores and on the small samples cut from the fabricated test slabs to CT Meter texture measurements on pavements and on the fabricated slabs. The additional experiment is described in section 5 of this thesis.

### **Sand Patch Test**

“The sand patch test (31) is a volumetric technique for determining the average depth of pavement surface macrotexture. A known volume of small particles (either sieved sand or small glass beads) is poured onto the pavement surface and spread evenly into a circle using a spreading tool. Four diameters of the circle are measured and an average profile depth is calculated from the known material volume and the averaged circle area. This depth is reported as the mean texture depth (MTD). The method provides an average depth value and is insensitive to pavement microtexture characteristics” (1). The sand patch test has been the standard macrotexture depth measuring technique against which newer methods and devices are compared (30, 32, 33, 34). The sand patch test is shown being conducted in Figures 4 and 5 . It can be seen in the photos that the technicians’ attention is focused on the pavement surface and not on the oncoming traffic. This can put the technician into a dangerous situation on the roadway if there is a lapse in the traffic control.



**FIGURE 4 Sand patch testing for pre-existing pavement macrotexture before chip sealing in Washington state: spreading glass beads into a circle.**



**FIGURE 5 Sand patch testing for pre-existing pavement macrotexture before chip sealing in Utah: measuring diameters of the circle of glass beads.**

### **Circular Texture Meter (CT Meter)**

The circular texture meter (CT Meter) (32), also known as the circular track meter, is used to measure and analyze pavement macrotexture using a charge coupled device (CCD) laser displacement sensor to measure surface elevations along a circular scanline on the pavement. The CT Meter equipment is shown in Figures 6 and 7.

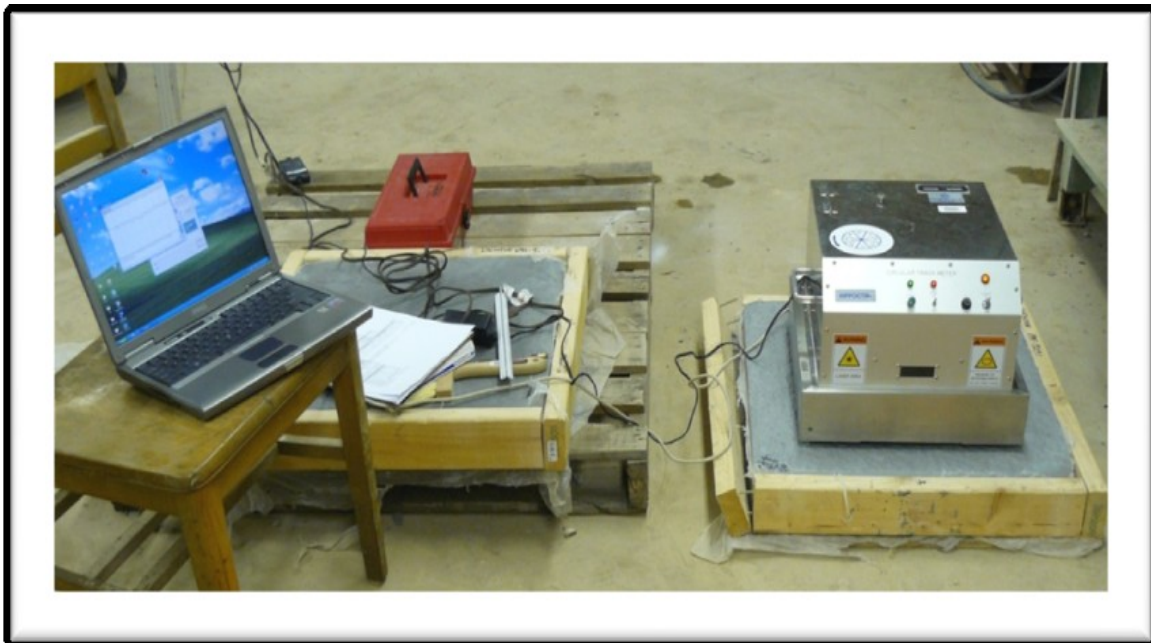


**FIGURE 6 CT Meter taking a macrotexture measurement on a fabricated test slab. CT Meter is connected to the laptop computer at the left for data collection.**



**FIGURE 7 A technician setting up the CT Meter in the field.**

In the CT Meter, the laser sensor is mounted on an arm on the underside of the instrument and follows a circular track with a diameter of 284 mm (11.2 inches). The laser beam spot size of the CT Meter is very small, and therefore it can discriminate each measuring point on the sample surface at a resolution that is high enough to capture the pavement macrotexture. Elevations on the pavement surface are measured and an elevation profile along the circle circumference is created. Data along the circumference are separated into eight segments. The CT Meter reports the mean profile depth (MPD) and the root mean square (RMS) for the entire profile, as well as those same values for each of the segments. With the circular scanline, four directions of data are obtained in one measurement, i.e., driving direction, perpendicular to the direction of travel, 45° to the direction of the travel, and the whole circumference. See Figure 8 for a schematic of the segments as they are related to the direction of travel of the traffic. Manufacturer specifications for the CT Meter include (32, 38):

- Laser beam spot size diameter: 70  $\mu\text{m}$  = 0.07 mm (0.0028 inch)

- Height of rotating arm above pavement surface: 80 mm (3.15 inches)
- Vertical resolution of the elevation measurement:  $3 \mu\text{m} = 0.003 \text{ mm}$  (0.0001 inch)
- Sample spacing of the measurements:  $0.87 \pm 0.05 \text{ mm}$  ( $0.0034 \pm 0.0020 \text{ inch}$ )
- Number of segments per scan: 8
- Segment length: 111.5 mm (4.39 inch) arc
- Diameter of the circular scanning profile: 284 mm (11.18 inches)
- Number of samples: 1,024 per revolution; 128 samples per segment
- Measurement time for one full revolution (one scan): approx. 45 seconds
- Power supply: an automobile battery (12V DC , 24W)
- Equipment dimensions: 400 mm (15.75 in.) long by 400 mm (15.75 in.) wide by 270 mm (10.63 inches) high, without the case
- Equipment weight (CT Meter, not including the computer): 13 kg (28.7 lbs) without the case, and 24 kg (52.9 lbs) with the case; fairly easily portable
- Data recording: laptop computer

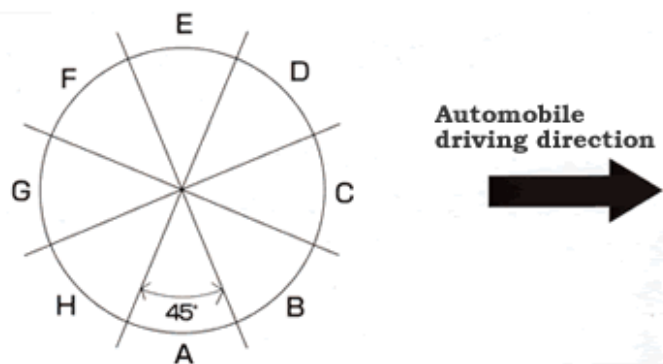


**FIGURE 8** The eight segments of the CT Meter's circular profile with direction of traffic shown (32).



### **Calculation of the MPD**

The method for calculating the pavement macrotexture MPD is described in ASTM E 1845-01, as follows: “The measured profile is divided for analysis purposes into segments each having a baselength of 100 mm (3.9 inches). The slope, if any, of each segment is suppressed by subtracting a linear regression of the segment. The segment is further divided in half and the height of the highest peak in each half segment is determined. The difference between that height and the average level of the segment is calculated. The average value of these differences for all segments making up the measured profile is reported as the MPD” (39).

### **Aggregate Imaging System (AIMS)**

The aggregate imaging system (AIMS) was created to quantitatively characterize aggregates (40). There have been several versions of the AIMS system during its development, but the system basically consists of a camera mounted above a table with several available lighting configurations and a computer. AIMS can be used to describe characteristics of coarse or fine aggregates. Coarse aggregate is characterized by particle shape, angularity, and texture. Samples of coarse aggregate are placed on the AIMS table under the camera and lighted from above, below, or both; and camera images are used to quantify the aggregate characteristics (1).

Surface texture is among the coarse aggregate characteristics which AIMS can characterize. AIMS is capable of quantifying surface texture of aggregates using two different methods: wavelet transform analysis of grayscale photos of the sample surface, and profiling of scanlines along the surface using the focal length of the lens to measure elevations along the scanline. The AIMS camera lens can adjust to different focal lengths and can therefore include different sizes of field of view of the sample surface. The focal length of each image is the average focal length for the included field of vision. By adjusting the focal length, AIMS can focus on different levels of texture, including

macrotexture and microtexture. AIMS was developed to quantify aggregate characteristics, including surface texture; but it could be used to quantify the surface texture of any sample that can be brought into the laboratory.

Analyzing macrotexture of coarse aggregates is comparable to measuring macrotexture of a pavement core or sample, as is demonstrated in this project.

### **AIMS Texture Analysis Using Grayscale Image Analysis and Wavelet Transforms**

AIMS can produce relative texture characterizations of a sample surface by creating grayscale photographs of the surface and then analyzing the images using a mathematical technique called wavelet transforms. This application of the AIMS was not utilized in this project. But it is presented here because of the potential for developing a portable and rapid measuring system which could use this technique for field investigation of roadway macrotexture for chip seal construction. A recommendation for further work on this topic is offered in this thesis.

Texture analysis of a photographic image attempts to quantify texture qualities described by terms such as rough and smooth from the photographic image. Regions in an image are characterized by their texture content as “a function of the spatial variation in pixel intensities” (41).

Texture analysis can be conducted using either black and white images or gray images. A disadvantage of using black and white images is that a high resolution is required for capturing the images, making it difficult to use automated systems. Another disadvantage is that texture details are lost when a gray image is converted to black and white. The analysis of gray images captures more texture data at the surface of a sample which leads to more detailed information about the surface texture. “However, the main challenge facing this technique is the influence of natural variation of color on gray intensities and, consequently, texture analysis. Some image analysis techniques have the potential to separate the actual texture from color variations” (42).

In a grayscale image, the surface irregularities manifest themselves as variations in gray-level intensities over a range. Large variations in gray intensity in a photograph represent a rough surface texture, whereas smaller variations in gray intensity result from a photograph of a smooth surface (43). AIMS characterizes the surface texture of aggregates with a “texture index”. The AIMS texture index for aggregates ranges from 0 to 800. A texture value of 500 or above is typical for a highly rough aggregate, and a texture value of 150 or below is typical for a polished aggregate (44).

AIMS uses wavelet transforms, a multiresolution analysis (MRA) technique, to analyze the photographic images of the aggregate surface. Wavelet transform is a mathematical process where an amplitude-time function is used to describe a wave and is then converted into an amplitude-frequency function for describing that same wave. Wavelet transform is similar to fast Fourier transform, but wavelet transform produces better resolution of waves at different frequencies (high versus low frequencies) than can be achieved with fast Fourier transform.

“Wavelet analysis is a powerful method for the decomposition of the different scales of texture (45). In order to isolate fine variations in texture, very short-duration basis functions should be used. At the same time, very long-duration basis functions are suitable for capturing coarse details of texture. This is accomplished in wavelet analysis by using short high-frequency basis functions [for the fine textures] and long low-frequency ones [for the coarse textures]. The wavelet transform works by mapping an image onto a low resolution image and a series of detailed images. The low-resolution image is obtained by iteratively blurring the original images, eliminating fine details in the image while retaining the coarse details. The remaining detailed images contain the information lost during this operation. The low-resolution image can further be decomposed into the next level of low resolution and detailed images” (40).

The grayscale image wavelet analysis capability of AIMS was not used in this project. It is presented here because of the potential for developing a portable and rapid system which could use this technique for field investigation of roadway macrotexture

for chip seal construction. Some discussion of this will be presented in the future recommendations of this thesis.

### **AIMS Texture Analysis Using Height Measurements and Profiling**

AIMS can also be used to measure macrotexture using a profiling technique that is similar to the profiling method used by the CT Meter. However, the CT Meter process depends on depth measurement using a laser beam; whereas the AIMS process depends on focusing and camera focal length to measure surface elevations. For this project, profiling of the sample surfaces was the procedure of interest from the AIMS system to be compared with results from the CT Meter and the sand patch test. In order to quantify macrotexture, the AIMS system was used to measure surface elevations along scanlines of the test slab surfaces at an appropriate focal length and field of view to capture macrotexture.

AIMS was developed in several steps, and therefore two versions of the AIMS equipment were available at TAMU. For this part of the project, the older AIMS equipment was utilized. This AIMS system can be seen in Figure 9.

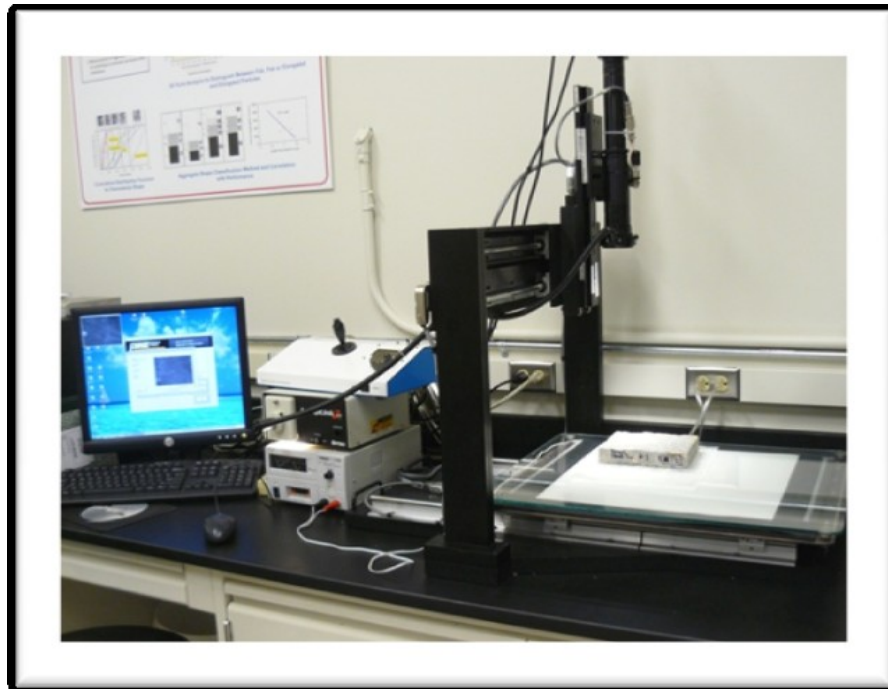


**FIGURE 9** The older version of the AIMS equipment is shown. Note that the table is stationary and the camera lens system moves to scan the sample(s) in a grid pattern. On the table can be seen one of the small samples that were cut from the fabricated slabs. The newer version of the AIMS equipment (which is shown in section 4 of this thesis) has a rotating table and a stationary camera lens system which is housed inside a black box to enhance control of the lighting.

The older AIMS equipment system scanned and measured elevations along parallel scanlines in which “depth measurements were generated every 1 mm for 4 scanlines of 100 mm length each, 20 mm apart, and in 2 perpendicular directions, for a total of eight scanlines per test slab. The total of eight scanlines at 100 mm length each was chosen to be similar to the eight segments of the CT Meter’s profile. The two sets of 4 scanlines each were taken in perpendicular directions to account for directional differences in pavement texture. This arrangement could be used to compare directional differences in texture, that is by texture in the direction of traffic versus texture perpendicular to the direction of traffic. Profiles were generated for the scanlines and

analyzed in a procedure similar to the CT Meter analysis, as described in ASTM's specification for calculating pavement macrotexture as MPD (39). A mean profile depth, MPD, similar to that from the CT Meter was calculated from the AIMS data for each of the three test slabs" (1).

The newer AIMS equipment system was used for the research described in section 5 of this thesis, that includes photographs of the newer AIMS system. The scanline configuration for the new AIMS equipment system differs from that described here for the old AIMS system, and will be described subsequently in section 5.

### **Ames Laser Texture Scanner**

The Ames laser texture scanner has recently been developed as a very portable piece of equipment for using a laser to measure macrotexture on pavement surfaces (46). Figure 10 shows a photograph of this equipment.



**FIGURE 10 Technician using the Ames laser texture scanner to measure pavement macrotexture (46).**

The Ames laser texture scanner was not used in the project for this thesis. However, it will be compared to the devices which were used in this project and will be considered in the thesis recommendations. This system “is designed to measure...two decades (2 inches to 0.02 inch) in the macrotexture waveband and one decade (0.02 inch to 0.002 inch) of the microtexture waveband (47)” (48).

The Ames laser texture scanner is a standalone unit containing a laser which scans the pavement surface in multiple parallel scanlines. The unit then calculates and stores index calculations, including the MPD and the RMS. The unit can render a three dimensional (3-D) image of the material surface. The scanner is capable of scanning an area that is 101.6 mm (4 inches) long and 76.2 mm (3 inches) wide; and within that area, the operator can choose the number of scanlines. It has a maximum capacity of 1200 lines, which would equate to an average spacing of 0.0635 mm (0.0025 inch) between scanlines. The laser has a dot size of approximately 0.050 mm, or 50  $\mu\text{m}$  (0.002 inch); this dot size allows the scanner to discriminate surface elevations in the macrotexture range and into the microtexture range (47, 48).

A study performed for the Ohio Department of Transportation, ODOT, (37, 48) compared methods for measuring pavement macrotexture, including the Ames laser texture scanner. The researchers ran preliminary tests with the Ames scanner in which they measured several macrotextures using 10, 100, and 1200 scanlines. They determined that running 100 scanlines per texture measurement provided the most stable MPD. This was more than the 10-30 scanlines per texture measurement recommended by Ames (48). “The use of a 100 line scan [was] deemed more appropriate due to ... the precision required for this experiment, since preliminary tests showed there to be little or no difference [in MPD] between the 100 and 1200 line scans” (48).

According to the manufacturers, the Ames laser texture scanner specifications include (46):

- Vertical sample resolution: 0.015 mm (0.0006 inch)
- Horizontal sample resolution: 0.015 mm (0.0006 inch)
- Profile wavelength: ranges from 0.03 mm to 50 mm (0.0012 inch to 2 inches)

- Laser dot size: approximately  $50\ \mu\text{m} = .050\ \text{mm}$  (0.002 inch); compare to the dot size of the CT Meter laser =  $70\ \mu\text{m} = 0.07\ \text{mm}$  (0.0028 inch)
- Standoff distance (distance of laser head above sample surface): 42 mm (1.65 inches)
- Horizontal sample spacing (distance between elevation measurements): 0.015 mm (0.00059 inch); spacing is smaller than the reported dot size of the laser. Compare to  $0.87 \pm 0.05\ \text{mm}$  ( $0.0034 \pm 0.0020$  inch) horizontal sampling spacing of the CT Meter measurements
- Scanline length: 100 mm (3.94 inches); compare to CT Meter segment length = 111.5 mm (4.39 inches)
- User selectable scanning resolution: from 1 to 960 scanlines
- Distance between lines at 960 scanlines: 0.08 mm (.0031 inch); therefore, distance between lines at 10 scanlines would be 8.47 mm (0.3333 inch); and distance between lines at 100 scanlines would be 0.77 mm (0.0303 inch)
- Time per set of measurements: 90 seconds/10 scanlines (1.5 minutes/10 scanlines)
- Power: high cycle rechargeable batteries; can provide up to one hundred scans per charge
- Data storage: data file in the instrument; can be easily downloaded to a PC through an Ethernet interface

The time needed to run 100 scanlines with the Ames scanner, as were run in the ODOT study, would be about 900 seconds (15 minutes) per texture measurement; this time is too long for the safety of the technicians out on the roadway. However, the Ames scanner could be used to run 8 scanlines, 4 parallel to the traffic direction and 4 perpendicular to the traffic direction as was done with the old AIMS system in this project; and this would take about 72 seconds, which is a rapid measurement and more safe for the technician to perform. In the AIMS measurements taken on the old AIMS system in this project, depth measurements were generated every 1 mm ((0.0394 inch)



for 4 scanlines of 100 mm (3.94 inches) length each, 20 mm (0.7874 inch) apart, and in 2 perpendicular directions, for a total of eight scanlines per test slab.

## **RESULTS AND ANALYSES**

For all of the texture analyses in this section of the thesis, the between-wheel path and the in-wheel path texture measurements were averaged to give an average texture depth of the pavement at each measurement location.

Sand patch testing has been a standard method in the past for measuring pavement macrotexture. Previous work suggests that there is a high correlation between the sand patch mean texture depth, MTD, and the CT Meter mean profile depth, MPD (34, 35). This correlation and the ease and speed of operation make the CT Meter an ideal method for measuring pavement macrotexture in the field during chip seal operations. Further correlation of macrotexture measurements with chip seal binder spray rates would provide a method for quantitatively adjusting binder spray rates to the pavement texture. A correlation was developed in the work done for this project at Colorado State University and is documented in the project final report (1).

To develop a regression equation between the results from the sand patch tests (MTD) and the results from the CT Meter measurements (MPD) for data from this project, data points of sand patch MTD versus CT Meter MPD measured at the same place on the pavement were plotted for each measurement location in the field (Figure 11). The resulting plot visually confirms that a linear relationship exists between the two measurements.

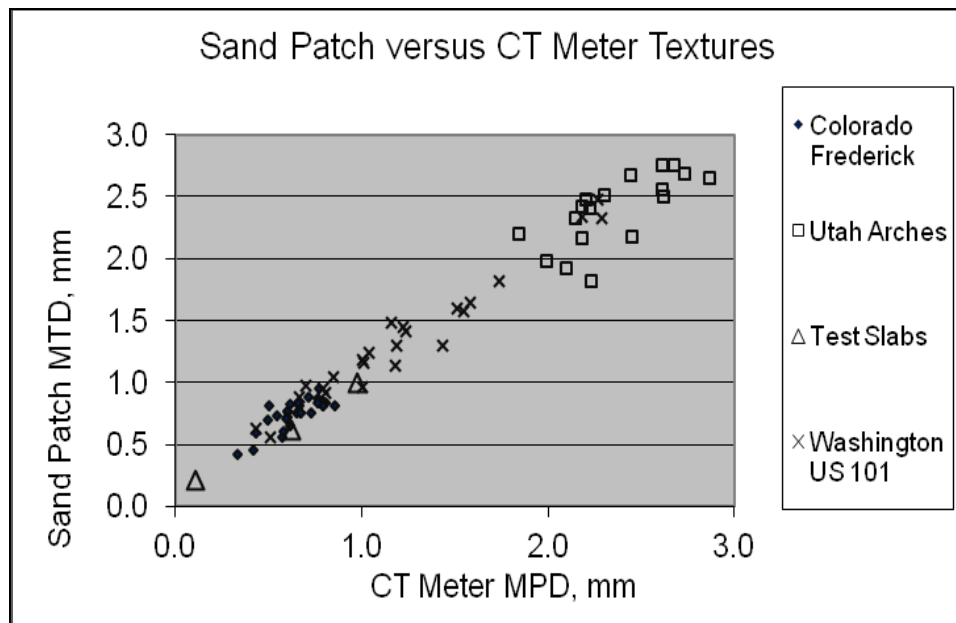


**FIGURE 11** Texture measurement results from NCHRP Project 14-17 chip seal sites at Arches National Park, UT; a county road in Frederick, CO; US 101 in Washington state; and 3 fabricated test slabs. Sand patch MTD versus CT Meter MPD data points are plotted for each measurement location (*I*).

A linear regression equation was then fitted through all of the data points (Figure 12), resulting in the following regression equation:

$$\text{Sand Patch MTD, mm} = 0.955 * (\text{CT Meter MPD, mm}) + 0.140 \quad (3)$$

The regression equation has a slope of 0.955 (close to 1, indicating an approximately 1:1 relation between the two measurement methods) and an  $R^2$  correlation coefficient of 0.97 (also close to 1, again indicating good correlation between the two measurement methods).

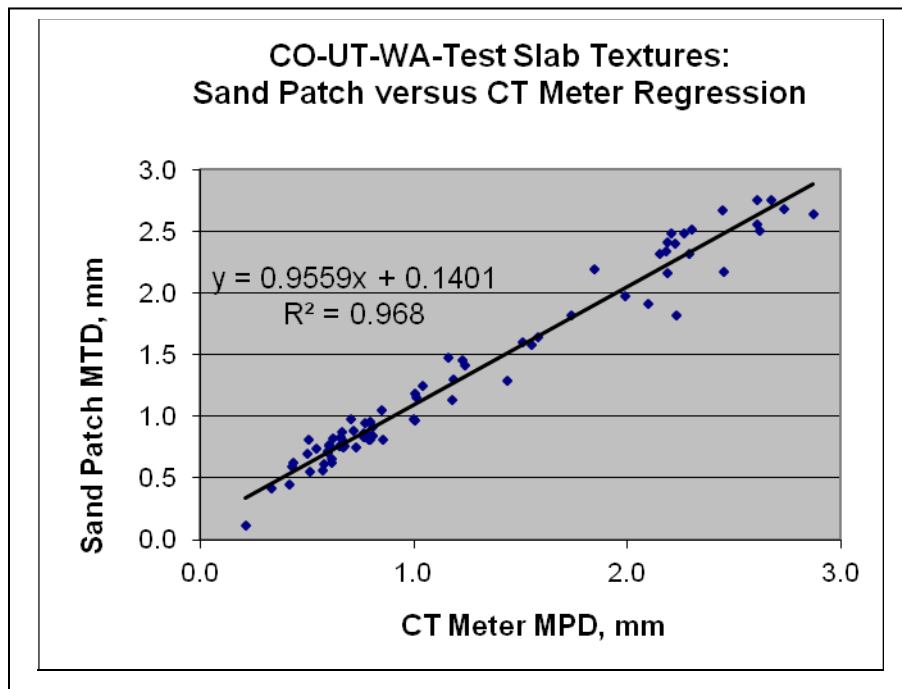


**FIGURE 12** Texture test results from NCHRP Project 14-17 chip seal sites at Arches National Park, UT; Frederick, CO; Washington state US 101; and 3 fabricated test slabs. Linear regression equation was fitted through the data points as shown.

Numerous linear regression equations have previously been developed to correlate CT Meter MPD to sand patch MTD (33, 34, 35). Table 4 shows some of the regression equations developed by other researchers along with the equation developed in this research. It can be seen that the equations are similar, again indicating strong evidence for a linear relationship between the MPD and the MTD parameters. All of the equations have slopes close to 1 and they also have intercepts close to 0, indicating a good 1:1 relationship between MPD and MTD.

**TABLE 4 Linear regression equations of sand patch MTD versus CT Meter MPD from various sources, including the regression equation developed from data in this project.**

<b>Source (Reference)</b>	<b>Linear Regression Equation</b>
NCHRP Project 14-17	$MTD = (0.955 \times MPD) + 0.140$
ASTM Spec. E 2157-01, Reapproved 2005 (32)	$MTD = (0.947 \times MPD) + 0.069$
Abe et al., TRR Volume 1764, 2001 (33)	$MTD = (1.03 \times MPD) + 0.15$
Hanson et al., NCAT, 2004 (2000 Test Track) (34)	$MTD = (1.0094 \times MPD) - 0.0056$
Hanson et al., NCAT, 2004 (2003 Test Track) (34)	$MTD = (0.9265 \times MPD) + 0.0633$

The regression equation developed from this project was also compared graphically to the regression equations from other publications, including the equation recommended in the ASTM CT Meter specification (32) (Figure 13). The regression equation developed in this project falls graphically between equations from other research projects and close to the equation shown in the ASTM specification.

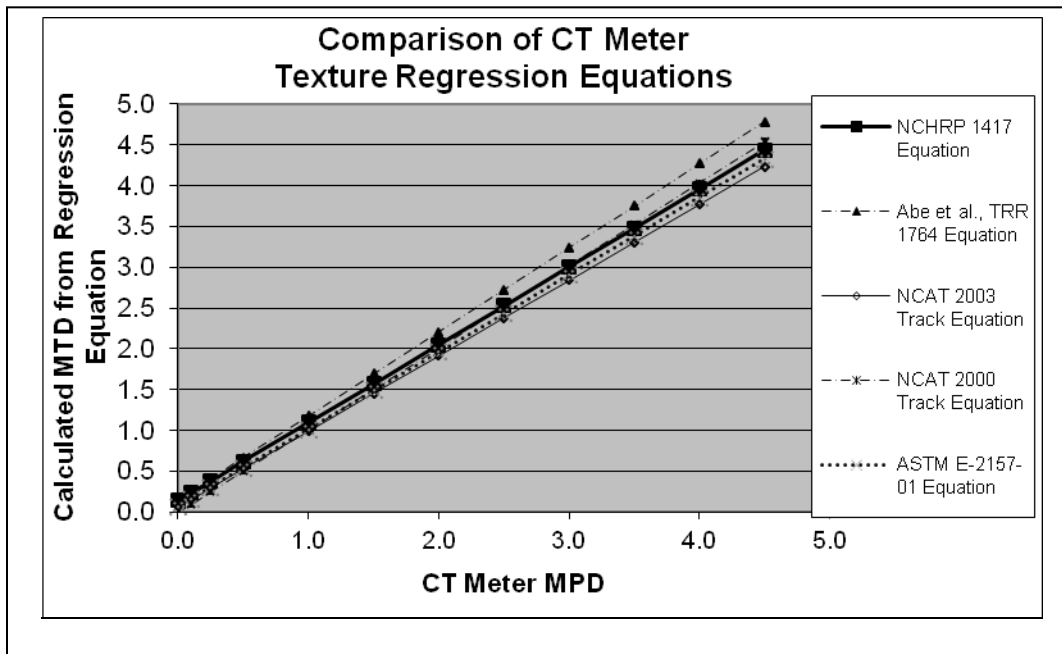


**FIGURE 13 Comparison of the regression equation from this project to the regression equations from other research. The regression developed from this project falls among the regressions from other research.**

The MPDs calculated using the AIMS on the test slabs were also compared to results from the other methods by developing linear regressions between AIMS MPD and CT Meter MPD measured on each of the three test slabs, shown in Figure 14, and between AIMS MPD and sand patch MTD measured on each of the test slabs, shown in Figure 15. The  $R^2$  correlation coefficients of these regressions are 0.87 and 0.93, respectively, again indicating high correlations between the measurement methods. These results suggest that the macrotexture profiling methods used by both the CT Meter and the AIMS to measure MPD can be used to predict the volumetric MTD of many textures.

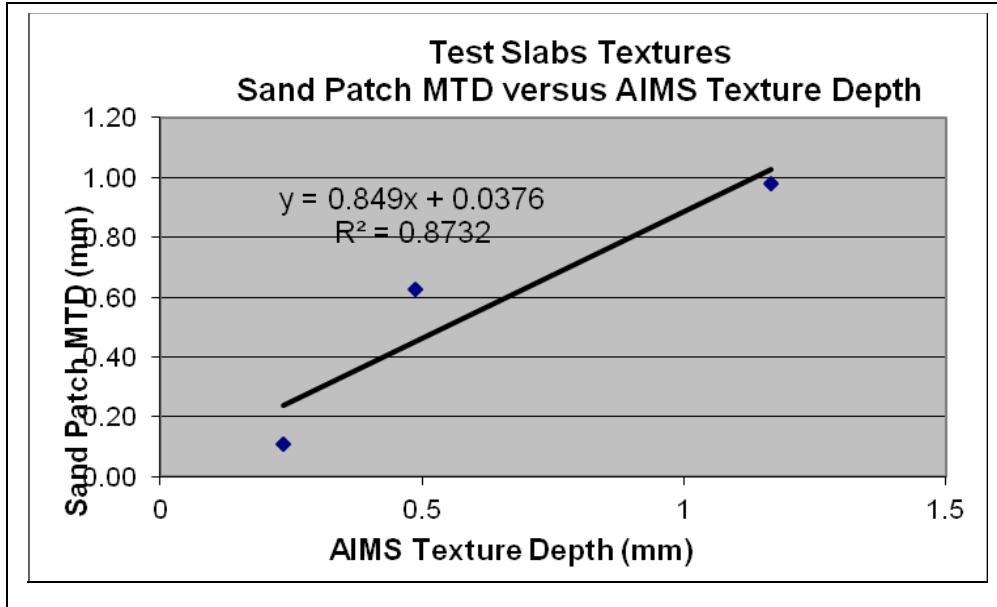


**FIGURE 14** Texture test results from NCHRP Project 14-17 test slabs: Sand patch MTD plotted versus AIMS texture depth, and linear regression equation fitted through the data points.

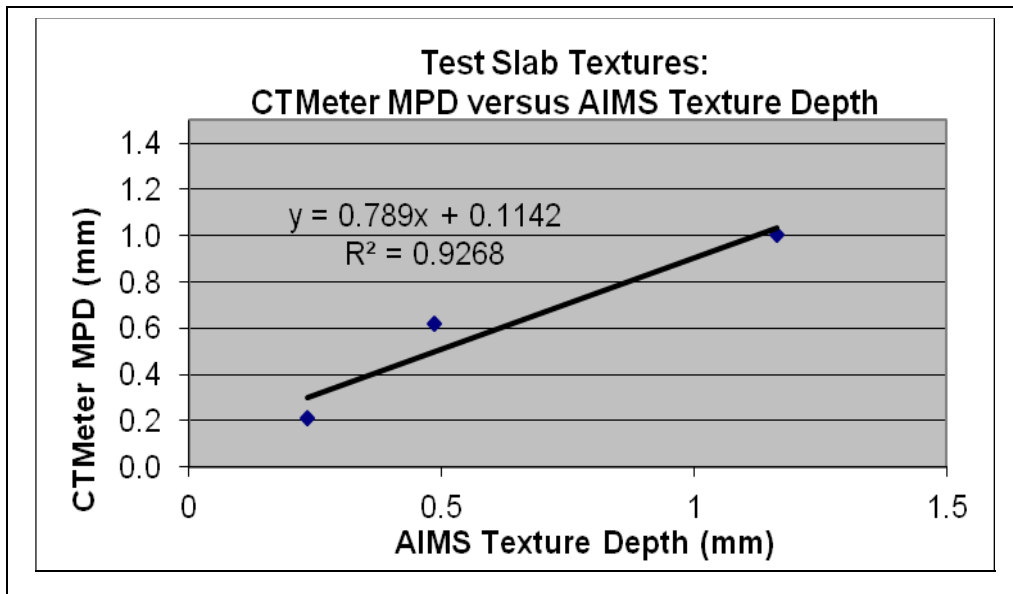


**FIGURE 15.** Texture test results from NCHRP Project 14-17 test slabs: CT Meter MPD plotted versus AIMS texture depth, and linear regression equation fitted through the data points.

Other researchers have suggested that the sand patch test method does not give good texture results for porous pavement surfaces (for example, open graded or porous friction courses) because the sand particles (or glass spheres) flow through the interconnected pores and out of the measuring area, thus giving an erroneous reading (34). The CT Meter measurements would not have the same difficulty because the laser measures depths at specific points along its profiling path; and therefore it is expected that the CT Meter could be used to measure texture of porous layers like open graded friction courses and porous friction courses.

It has been observed by other researchers that there is more variability in the MPD results from CT Meter texture measurements than there is in the MTDs from sand patch tests (34). It is expected that there is more variability in the profile along a circumference than there is in texture from a volume of an entire circle that is approximately the same diameter as the CT Meter scan. The CT Meter variability is not due to variability in the measuring capability or accuracy of the CT Meter itself, but to the more accurate measurement of a more variable parameter, i.e. exactly where the circumference is located on the pavement surface. CT Meter measurements and resulting parameters can be duplicated with high reproducibility when the meter is not moved between successive measurements. CT Meter measurements vary when the instrument is moved by as little as an inch between successive measurements. This indicates slight variability in the pavement macrotexture from place to place. In this project, CT Meter measurements were always taken in pairs with a slight movement of the CT Meter, about 25.4 to 50.8 mm (1 to 2 inches), between the measurements in the replicates.

## **CONCLUSIONS, RECOMMENDATIONS, AND FUTURE RESEARCH**

Based on the results from this project, this thesis recommends the use of the CT Meter for assessing existing pavement macrotexture to use in adjusting emulsion spray rate in a chip seal operation. The CT Meter measures surface heights and generates a profile along the circumference of a 284 mm (11.18 inches) diameter circle, and then

calculates an MPD from the heights. The CT Meter equipment is expensive, but taking the CT Meter measurement can be accomplished more quickly than a sand patch measurement can be made. Also, the technician's attention is not as focused on the pavement surface and so the technician can be more aware of the traffic. This makes the measurement using the CT Meter safer than the sand patch measurement as it exposes the technician to less accident risk. The CT Meter is a more expensive piece of equipment than the items needed to make a sand patch measurement; but the increase in safety to the technician warrants the CT Meter expense.

There is a new and alternative laser texture measuring device, the Ames laser texture scanner, being investigated in other research (40) which has been shown to produce acceptable macrotexture evaluations when compared to measurements made with the sand patch method and with the CT Meter. The Ames device is smaller and lighter than the CT Meter, making it easier to transport and use. The Ames scanner produces scanlines 100 mm (3.94 inches) long, similar in size to the 111.5 mm (4.39 inch) arc segment length of the CT Meter. The Ames device scanlines are taken all in one direction; but the instrument can easily be set to take 4 scanlines in one direction and then turned 90 degrees to take 4 additional scanlines, similar to the scanline configuration used by the old AIMS device that was used in this research project. This would also produce a total scanline size similar to the total scanline of the CT Meter.

The study completed at Ohio State University for ODOT compared MPD from the Ames device to MTD from the sand patch test (48) and found the following linear correlation:

$$\text{Sand Patch MTD} = 1.1743 * (\text{Ames MPD}) - 0.00005, R^2 = 0.9844 \quad (4)$$

Equation 4 indicated a close correlation between the MPD from the Ames laser texture scanner and the sand patch test MTD. Therefore it is expected that the Ames device would be an effective alternative to the sand patch test and to the CT Meter for measuring pavement macrotexture, especially directly before a chip seal operation.



Some macrotexture researchers (49) have stated that the laser devices are not useful for measuring pavement textures for chip seals because they measure along a circumference instead of taking a volumetric measurement. However, the CT Meter MPD has had a good correlation in many studies with the sand patch MTD. In addition, the Ames laser device could be used to quickly measure a grid of elevations which could approximate a volumetric measurement. This would be similar to the way that a great number of pixels in a photograph blend together to form what appears to be a solid picture.

The AIMS is laboratory equipment which needs road cores or laboratory samples to measure pavement texture and therefore is not immediately useful for measuring pavement macrotexture for chip seal construction. However, the AIMS MPD also compared well in this research to the CT Meter MPD. It is recommended that, if the AIMS profiling technique could be developed within a portable device, this could be effectively used for macrotexture measurement prior to chip seal construction. However, one issue with this might be that the profiling would take too long to be safe for the technician out on the roadway.

Other researchers have investigated the use of photographic image analysis to quantify macrotexture of pavement surfaces in the field (49). This analysis method, which used fast Fourier transform of black and white images and looked for aggregate edges in asphalt binder background (white on black), is similar to that used for the grayscale image analysis in the AIMS system. A similar camera system could be developed which uses wavelet analysis of grayscale images instead of fast Fourier transform analysis of black and white images. If this method proved to be successful, it could provide another viable, rapid, and relatively inexpensive alternative to the sand patch test MTD and the CT Meter MPD.

## 5. A SIMPLE LABORATORY METHOD FOR MEASURING PAVEMENT MACROTEXTURE USING PAVEMENT CORES AND THE AGGREGATE IMAGING SYSTEM (AIMS)<sup>5</sup>

### INTRODUCTION

Pavement surface friction is a key factor influencing traffic accident rates and, consequently, road safety (30). This is especially evident when pavements are wet. Pavement surface texture governs most tire/pavement interactions (50) and is a major contributor to pavement surface friction characteristics. Measurement and analysis of pavement surface texture using a rapid and precise procedure which captures the pertinent effects in a safe manner is currently a subject of much interest. Emerging new technologies such as digital imaging are providing opportunities for new texture measurement methods; but these need to be fully investigated and correlated to each other in order to be used effectively.

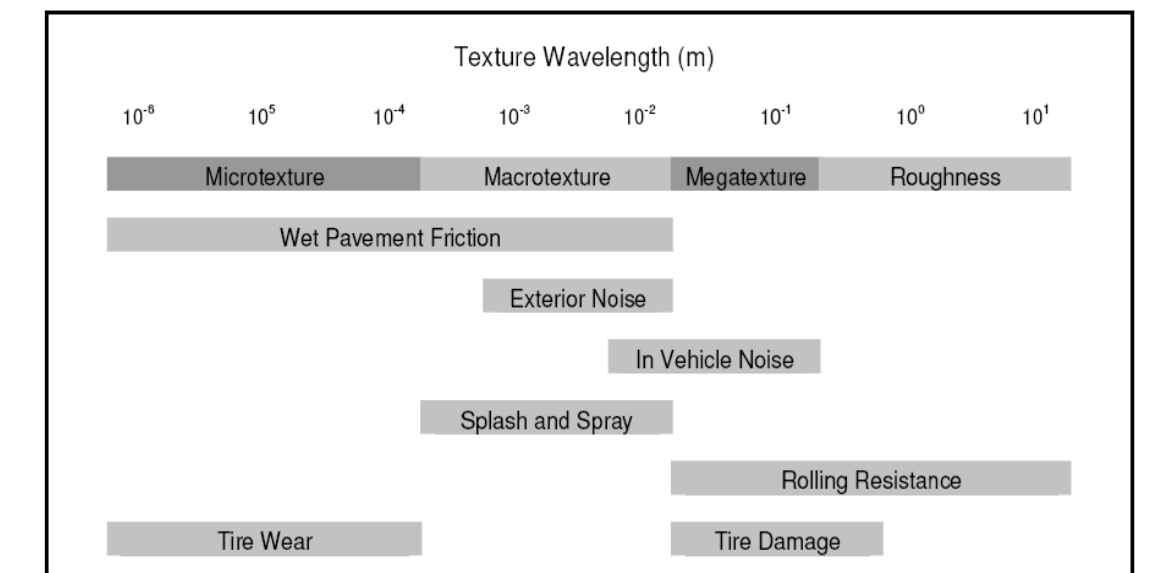
Pavement surface texture is comprised of combinations of the texture characteristics of feature depth (amplitude) and feature length (wavelength). Pavement texture has been divided into three categories based on the wavelength of its peaks: microtexture, macrotexture, and megatexture. Each of these categories affects different pavement properties. Figure 16 (30, 51) shows different categories of pavement texture and corresponding tire-pavement interaction effects.

Figure 16 shows that wet pavement friction is mostly affected by microtexture and macrotexture. Surface asperities less than 0.5 mm (0.02 inch) in height are classified as microtexture, while asperities greater than 0.5 mm (0.02 inch) in height are considered

---

<sup>5</sup> Paper presented at the 90<sup>th</sup> Annual Meeting of the Transportation Research Board, January, 2011, Washington, D.C., and published in the 2011 series of the *Transportation Research Record: Journal of the Transportation Research Board* (8). Copyright, National Academy of Sciences. Reproduced with permission of the Transportation Research Board.

macrotexture (52). Microtexture refers to irregularities in the surfaces of the aggregate particles (fine-scale texture) that are measured at the micron scale of coarseness and are known to be mainly a function of aggregate particle mineralogy (53). Macrotexture refers to the larger irregularities in the road surface (coarse-scale texture) that are associated with spaces between aggregate particles. The magnitude of this component of texture will depend on the size, shape, and distribution of coarse aggregates used in pavement construction, the nominal maximum size of aggregates, and the particular construction techniques used in the placement of the pavement surface layer (53).



**FIGURE 16 Pavement texture wavelengths and their associated tire-pavement interaction effects (30, 51).**

There is currently no way to directly measure pavement microtexture in the field. However, agencies use different methods for measuring macrotexture for use in maintenance and safety evaluation of pavements. Pavement macrotexture is traditionally measured using a simple and inexpensive volumetric technique called the sand patch test (31). But the safety of the technician performing the sand patch test on a pavement with

traffic is a concern because of the time and attention that it takes to do the test. Even with proper traffic control, the technician can be exposed to traffic hazards. Also, the results of the sand patch test can be influenced by the technique and skill of the technician performing the test. Alternatively, use of the circular texture meter (CT Meter) (32), a laser beam device for measurement of macrotexture, has provided a safer, more repeatable, and more reproducible technique than the sand patch test for measuring pavement macrotexture in the field because it is instrument-driven. It is not only faster and more precise than the sand patch test, but also the attention of the technician is not as focused on the pavement. However, there are still safety concerns in doing any field measurement; and environmental and pavement conditions may lead to erroneous interpretation of data. Recently high speed macrotexture profilometers have been developed which collect pavement texture data while traveling at highway speeds, eliminating the need for traffic control; however, these systems are expensive and require skilled operators for data collection and processing (52).

An instrument-driven pavement texture measurement that can be performed on a pavement core in the laboratory would be safer for the technician and may be more accurate and reproducible than field tests. Although a coring operation on the road is a time consuming process which exposes the coring technician to traffic, cores are sometimes taken anyway for purposes such as quality control of the materials and the construction procedure. These same cores could be used for non-destructive pavement texture measurement in the laboratory before other tests are performed.

The aggregate imaging system (AIMS) is an assemblage of laboratory digital imaging equipment that was developed for assessing the characteristics of shape, angularity, and surface texture of fine and coarse aggregates. AIMS may also be utilized to measure surface texture on pavement cores. The AIMS equipment configuration includes a digital camera that captures images at different resolutions, encompassing different fields of view, and using different lighting. The AIMS is a rapid, simple measurement system, and previous research studies have shown that the results are repeatable and reproducible (43, 54).

This paper describes the method and results of an experiment which compared texture measurements of pavement surfaces in the field using a CT Meter to texture measurements on pavement cores in the laboratory using AIMS. The results of statistical analyses on the measurement results were used to formulate recommendations for using AIMS to measure surface texture on field cores and for using the AIMS laboratory measurements to estimate the pavement surface texture.

## **OBJECTIVE**

The objective of this research study was to investigate the use of AIMS as a laboratory technique for measuring pavement texture as an alternative to field measurement of surface macrotexture of pavements. In order to achieve this objective, the following tasks were performed:

Task 1: Select field pavement sections with different macrotexture values and measure the macrotexture in the field using the CT Meter

Task 2: Obtain cores from the field sections and fabricate additional laboratory specimens with a range of macrotextures

Task 3: Use AIMS to measure surface texture of laboratory samples and field cores using different measurement scenarios

Task 4: Analyze the data and relate the field measurements using CT Meter and the laboratory measurements using AIMS

Task 5: Optimize the measurement scenarios and recommend a laboratory measuring technique for pavement texture using AIMS

## **METHODOLOGY**

### **Procedure**

Five different asphalt concrete pavement sections were selected, and the pavement macrotexture was measured on these field sections using the CT Meter.

Pavement sections were located on US-84 and IH-20 and had Texas Department of Transportation (TxDOT) Type C and Type D mixture designs (55). Because texture varies across the pavement, texture measurements were taken inside and outside of the wheelpath and on the shoulder. Thirteen cores were taken from all of the field sections and brought to the laboratory for further measurements.

In order to have a larger number of laboratory samples and a wider range of macrotexture values than was provided by the available pavement cores, additional fabricated samples from a previous project were included in this study. These additional samples were three concrete slabs which were the negative images of three asphalt concrete pavement sections of varying texture. The fabricated slabs were cast by pouring a very low viscosity self-consolidating Portland cement concrete into 45.72 cm by 45.72 cm (18 inch by 18 inch) forms on three different pavement surfaces. Self-consolidating concrete was used to make the specimens because of the concrete's ability to flow into the smallest spaces in the surface of the asphalt pavements. This created texture specimens that mimicked the texture of three pavement surfaces ranging from very rough, created from a highly raveled and pocked surface, to very smooth, simulating a very flushed surface (1). The surface textures of the three fabricated slabs were measured using a CT Meter. Then, three small samples, each approximately 15.24 cm x 15.24 cm (6 inches x 6 inches), were cut from each of the three fabricated slabs, providing nine total small slab samples for texture measurement with AIMS. Figure 17 shows a fabricated concrete slab with the CT Meter. Figure 18 shows three small slab samples with smooth, medium, and rough textures.



**FIGURE 17** Fabricated concrete slab with rough surface texture being measured by the CT Meter. The diagram of the circumferential segments into which the data are divided can be seen on the top of the CT Meter.

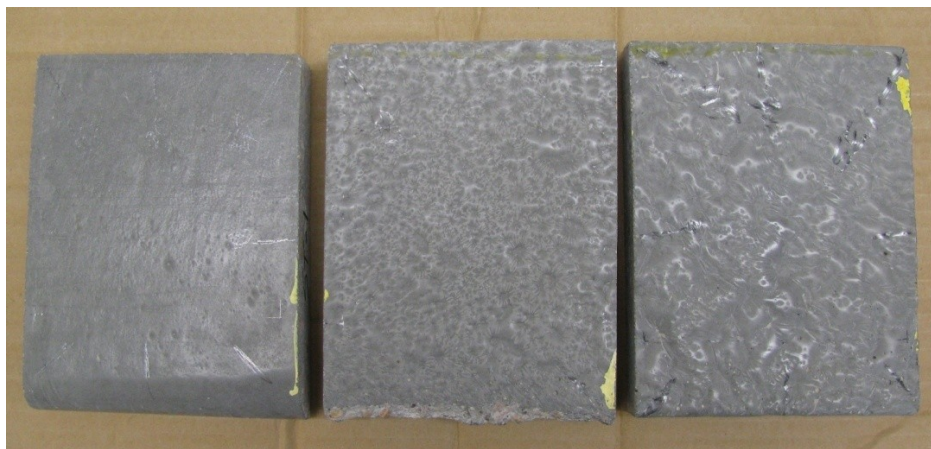


**FIGURE 18** Three 15.24 cm x 15.24 cm (6 inches x 6 inches) small slab samples with smooth, medium, and rough (left to right) textures cut from negative-image slabs cast on asphalt concrete pavement surfaces.

The texture results from the CT Meter and AIMS were analyzed and compared. A comprehensive statistical analysis was performed, and the relationships between the results of the different testing methods were studied. A simple linear regression between the results of the image processing technique (AIMS) and the laser measurement technique (CT Meter) was developed using the results from the three test slabs and ten of the cores. Then the predictive strength of the linear correlation was assessed using measurements made on the remaining three cores.

### **Texture Measurement Methods**

#### *Circular Texture Meter (CT Meter)*

The CT Meter test method is commonly used to measure and analyze pavement macrotexture with a laser displacement sensor (32). The laser sensor, with a laser beam spot size of 70  $\mu\text{m}$  (0.00276 inch), is mounted inside a box on an arm which follows a circular track 284 mm (11.2 inches) in diameter. Heights are measured along the circumference of the circle at a sample spacing of  $0.87 \pm 0.05$  mm ( $0.0343 \pm 0.002$  inch).

For analysis, the circumferential scanline is segmented into eight 111.5 mm (4.39 inch) arcs containing 128 measurements each (32). In order to calculate the mean profile depth (MPD) value, the height of the highest peak in each half-segment is determined, and the average of those two heights is the mean segment depth. The average of the mean depths for all eight segments is reported as the mean profile depth (MPD) for the entire circular profile. The calculation procedure is delineated in ASTM E 1845-01 (39). This MPD from the CT Meter has previously been highly correlated with the volumetric texture measurement from the Sand Patch Test, the Mean Texture Depth or MTD (32).

The root mean square, RMS, a statistical parameter for comparing relative sizes of data, is also reported by the CT Meter for the circumferential scanline height data. The RMS value for each direction can be calculated as:



$$RMS = \sqrt{\frac{\sum_{i=1}^n h_i^2}{n}} \quad (5)$$

where  $h_i$  is the height after sample slope adjustment for each individual measurement and  $n$  is the total number of measurements taken along the corresponding scanline. Thus, the RMS value considers all height measurements while the MPD first selects the maximum height in each half segment before averaging.

For this research, CT Meter MPDs were measured on the three fabricated slabs and at the coring locations in the five pavement sections that the cores were extracted from. The CT Meter MPDs are referred to in this study as  $MPD_{\text{field}}$ .

#### *Aggregate Imaging System (AIMS)*

AIMS was developed to quantitatively describe the characteristics of aggregates such as form, angularity, and microtexture (43, 56, 57). Currently, AIMS can also be used to quantify macrotexture of surfaces using the focal length of the camera over the viewing image in the lens. The AIMS system is equipped with a digital camera that has 5 different zoom ratios which capture a wide range of surface heights without changing parts. This camera is mounted above a wide rotating tray on which the specimens are placed. There are several lightning arrangements available including overhead and back lighting (57, 58). A photograph of the AIMS system showing the camera lens, overhead lighting, and rotating specimen tray is shown in Figure 19.

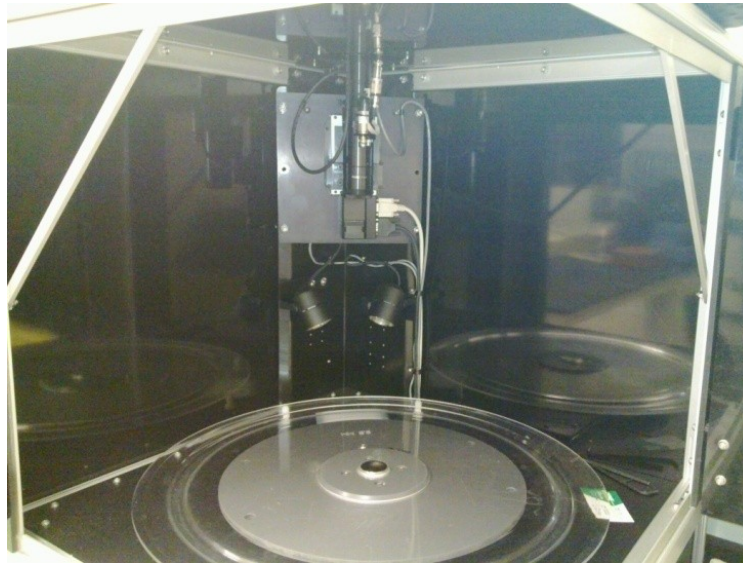


**FIGURE 19** Photograph of the inside of the AIMS system showing the camera lens (top), overhead lighting (middle), and rotating specimen tray (bottom).

Samples or cores are placed on the AIMS table under the camera and lighted from above for surface macrotexture scanning. The height is measured by first focusing the microscope on the lighting table and recording its location on the z-axis as the zero or reference point. Then, the microscope is moved up to take a gray image of the core surface. To achieve this, the digital camera moves upward until a high frequency signal from the microscope is received indicating that a high-resolution gray image is detected. The difference between the new location of the microscope and the zero point gives a texture height. The table rotates slowly and numerous measurements are made along a scanline. The ability of AIMS to measure the height of the specimen and to generate a profile of heights along a scanline allows it to be used as a macrotexture measuring device for field cores. Such a feature has been provided with the new version of the AIMS equipment (57, 58).

According to the new AIMS manual (58), the AIMS system scans the surface of the core or specimen five times. Each scan will capture images at a different magnification level (15.8, 12.60, 6.27, 3.13, and 1.2) across the entire core diameter. The first scan is at the maximum magnification level of 15.8. At this level, the photographic

image size for each individual height measurement is approximately 2.21 mm by 2.21 mm (0.097 inches by 0.097 inches) per image. Figure 20 shows an AIMS grayscale image at zoom level 15.8 on a small slab sample. During this scan the surface height of the specimen is measured at each image by focusing the lens on the sample surface. The heights produce the scanline profile that is analyzed to determine the MPD (58). Figure 21 shows a pavement core being scanned by AIMS.

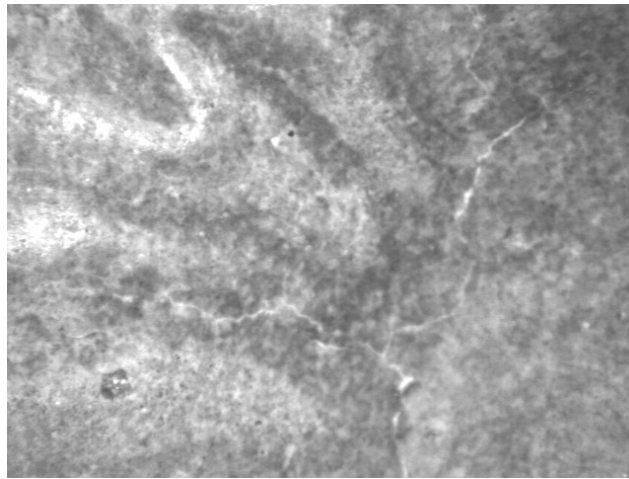


**FIGURE 20** AIMS grayscale image at zoom level 15.8 on a small slab sample.



**FIGURE 21** Pavement core during scanning in AIMS.

In the course of this research study, for each core, surface scanlines were run along each of 4 intersecting diameters for the entire diameter of the core, as shown and labeled in Figure 7. In the current configuration of the AIMS equipment, each scanline follows a slight arc because the AIMS table is a large rotating circle (which can be seen in Figures 19 and 21). However, the arc of the scanline is slight and the scanline is approximately linear.

The small slab samples were placed on the AIMS table in the same position as the cores, and the scanlines were run in a configuration as shown in Figure 22. On each of the small slab samples, two scanlines were run perpendicular to and centered along each edge, and two scanlines were run diagonally to each corner.

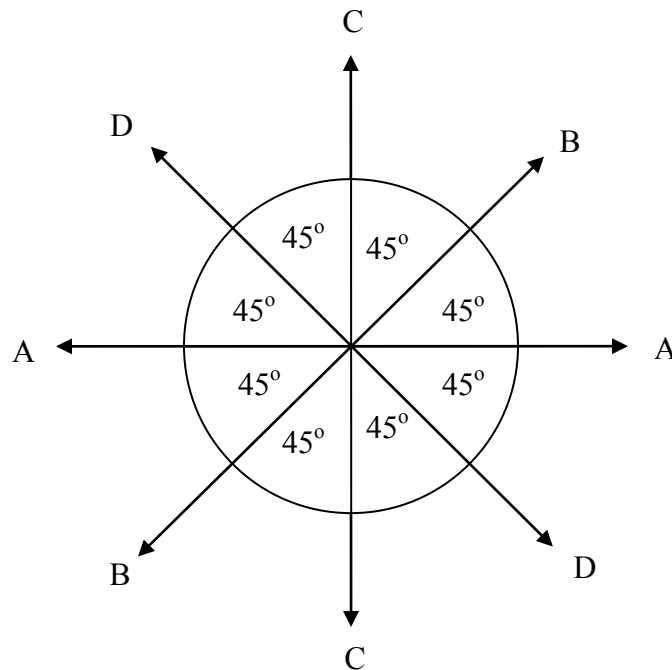


**FIGURE 22 Layout of the laboratory sample measurement directions.**

Texture profiles were generated for each of the scanlines. These profiles were divided into segments and analyzed in a procedure similar to that developed for the CT Meter analysis and described above (ASTM E 1845-09) (39). A MPD was calculated

from the AIMS data for each of the 13 pavement cores and the nine small slab samples. The AIMS MPDs are referred to as  $MPD_{lab}$  in this study.

## **RESULTS AND DISCUSSION**

In order to determine the relationship between AIMS measurements ( $MPD_{lab}$ ) and CT Meter measurements ( $MPD_{field}$ ), the MPDs from AIMS and the CT Meter were analyzed and compared using the statistical software SPSS<sup>®</sup>, Statistical Program for the Social Sciences (59).

### **Theoretical Background for the AIMS Analysis**

In the AIMS testing, each sample was rotated and scanned four times, and heights for creating a surface profile were measured along each scanline shown in Figure 7. The scanline profiles were divided into segments and MPDs were calculated as described above.

Using the 15.8 zoom level (which is the highest magnification level), the digital images were taken approximately every 2 mm (0.078 inch) and about 68 data points were available for each 152 mm (6 inch) scanline. Sample profiles of the three different textures from the small slab samples (smooth, medium, and rough) are shown in Figure 23.

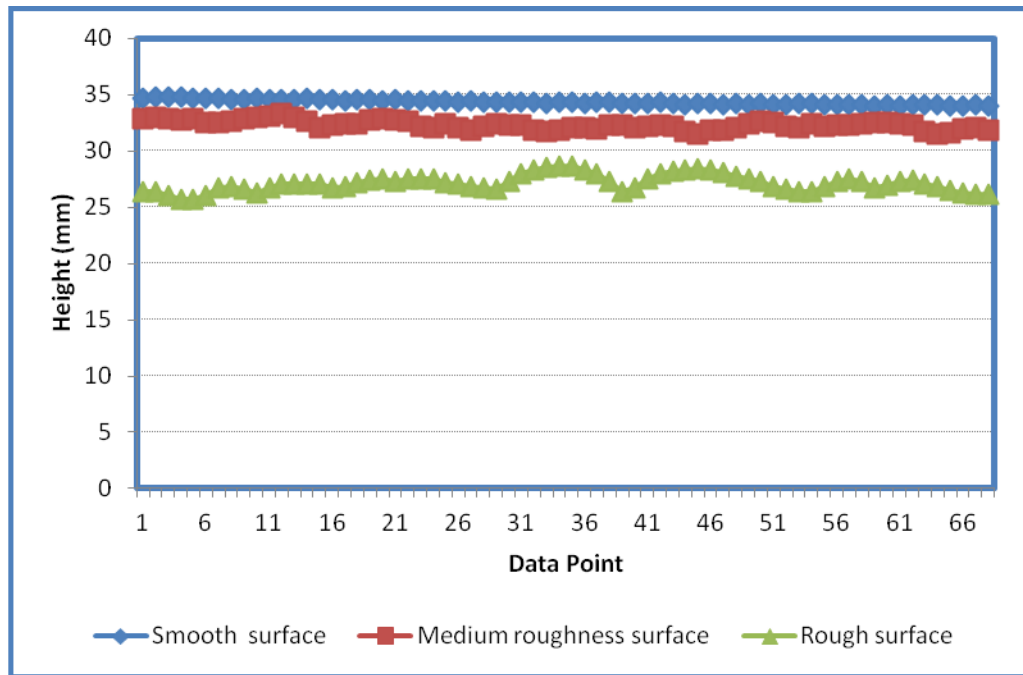
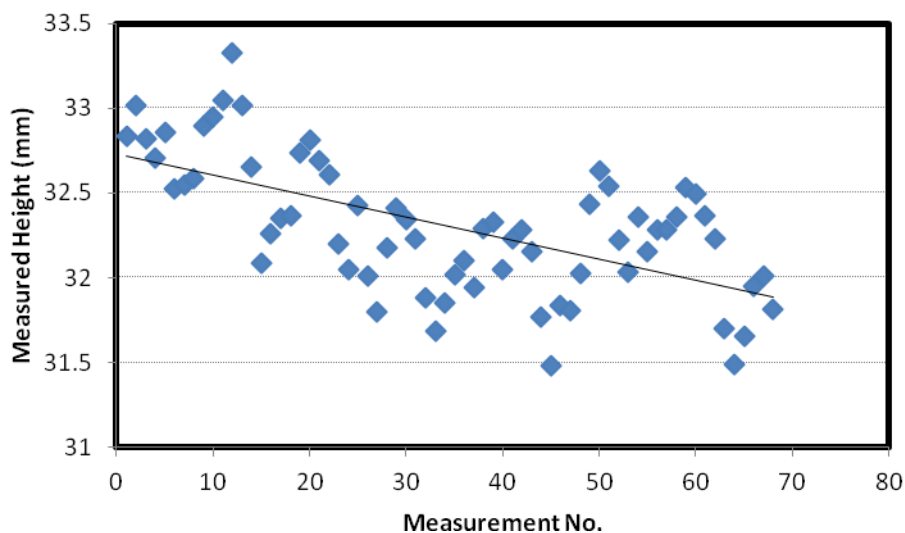
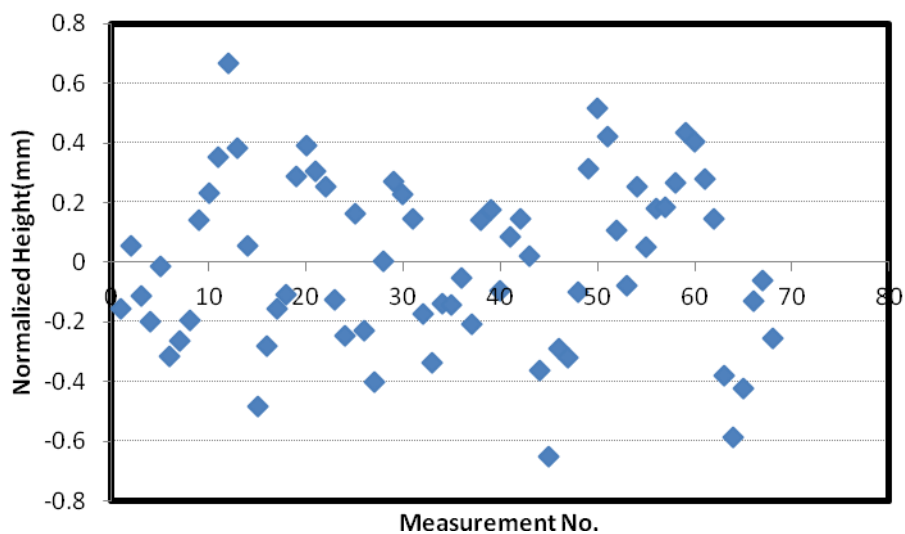


**FIGURE 23 Sample scanlines (of six inch segment lengths) showing profiles of the three different textures from the small slab samples (smooth, medium, and rough).**

It is probable that the core or small slab sample being measured has a sloped surface, i.e. that it is not cut flat or lying flat on the AIMS table. This surface slope must be removed from the scanline profiles so that the surface texture is measured from a level surface. Therefore, in order to suppress the slope of each sample a simple linear regression was performed to find the plane of the surface (Figure 24(a)), and the results were subtracted from measured heights for each sample. This provided a zero mean profile in which the area above the reference height is equal to the area below it (Figure 24(b)) (39).



(a)



(b)

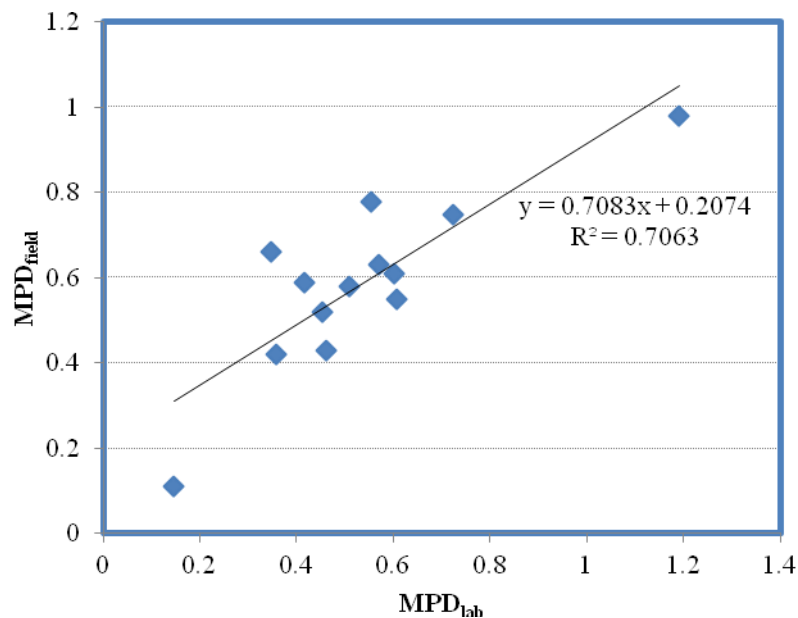
**FIGURE 24 Removal of specimen slope from AIMS scanlines showing: (a) Measured heights and linear regression; (b) Normalized heights with regressed surface line at zero.**

Then the mean profile depth (MPD) and the root mean square (RMS) ( $6\theta$ ) were calculated for each scanline (or direction). Thus, for each core or small slab sample, there

is an  $MPD_{lab}$  and an RMS for each of four scanlines (and for each of four scanned directions) as shown in Figure 14.

### The Relationship Between AIMS (Laboratory) MPD and CT Meter (Field) MPD

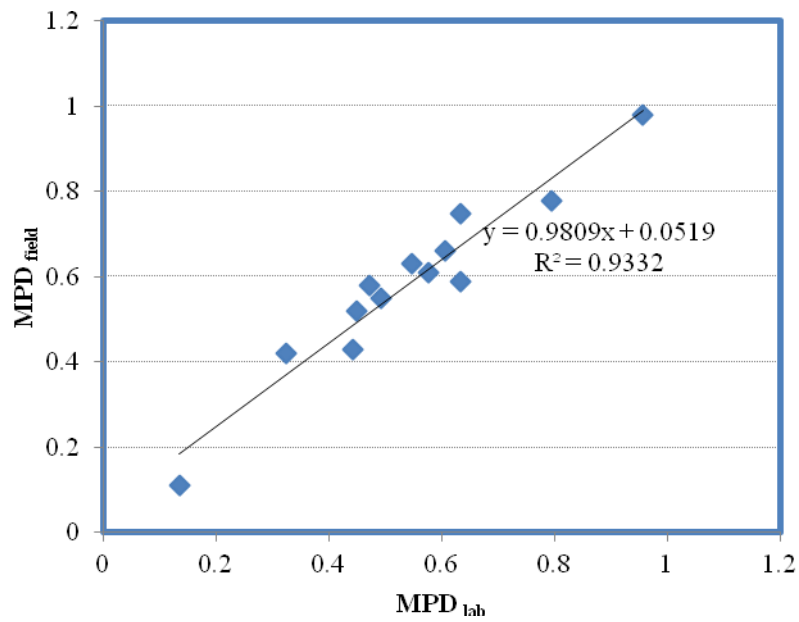
In order to investigate the effect of segment length used for analysis of the AIMS macrotexture, three different segment lengths were considered in the data analysis: 25 mm (one inch), 50 mm (two inch), and 75 mm (three inch). The  $MPD_{lab}$  value using each of these segment lengths was calculated similarly to the method described in ASTM E 1845-01 (39); and this  $MPD_{lab}$  was plotted against the CT Meter  $MPD_{field}$  for 10 of the 13 pavement cores and for an average of the three small slab samples from each fabricated slab. A linear regression was then calculated for each segment length, as shown in Figure 25.



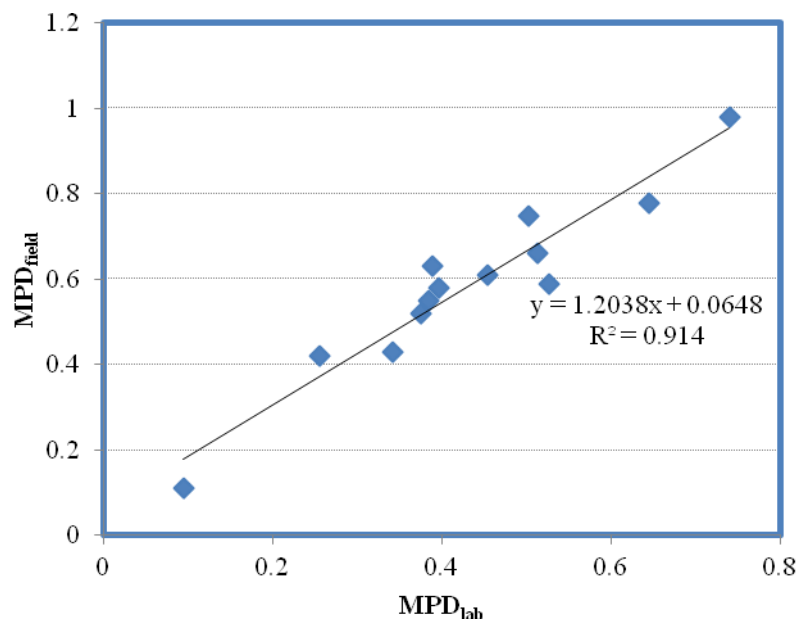
(a) Three inch (75) mm segment length.

**FIGURE 25** The relationship between lab (AIMS) and field (CT Meter) MPD values for different segment lengths: (a) Three inch (75) mm, (b) Two inch (50 mm), (c) One inch (25mm).





(b) Two inch (50 mm) segment length.



(c) One inch (25mm) segment length.

FIGURE 25 Continued.

Based on the regression models developed in Figure 25, the AIMS MPD values for three verification field cores were input into the regression equations as  $MPD_{lab}$ . The field texture values that were predicted from the regression equations were compared to the measured values from the CT Meter, as shown in Figure 26. Figure 26 indicates that analysis using scanlines divided into 50 mm (2 inch) segments accurately predicted the  $MPD_{field}$  values of the test cores with a minimum mean square error of 0.004. The mean square error of 75 mm (three inch) and 25 mm (one inch) segment lengths was 0.02 and 0.006, respectively.

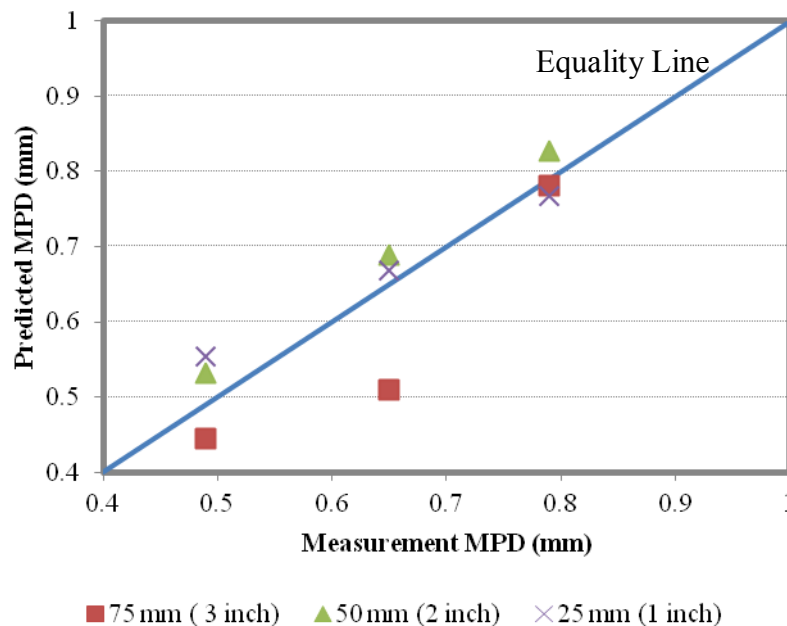


**FIGURE 26 Relationship between predicted MPD (from AIMS and regression equation, for three segment lengths) and measured MPD (from CT Meter) for the three verification pavement cores.**

Based on the results of the statistical analysis, selecting the 50 mm (two inch) segment length for calculating MPD based on AIMS measurements gives an accurate estimation of field (CT Meter) MPD values. Thus the recommended regression model for calculating a field value ( $MPD_{field}$ ) from the laboratory-measured value ( $MPD_{lab}$ ) (Figure 16(b)) is:

$$\text{MPD}_{\text{field}} = 0.98\text{MPD}_{\text{lab}} + 0.051 \quad R^2 = 0.93 \quad (6)$$

An AIMS MPD value calculated based on 50 mm (2 inch) segment lengths was selected as representative of the surface macrotexture, and further statistical analysis was performed to determine if this value was sensitive to different textures and to direction. The small slab specimens with smooth, medium, and rough texture were selected for this analysis because it was known that they were significantly different from each other in terms of their texture values; and one-way analysis of variance (ANOVA) was performed. The results of the analysis showed that the difference between different textures is statistically significant at a 0.05 significance level ( $\alpha = 0.05$ ), and therefore the AIMS measurement method is statistically able to distinguish between three different texture levels. The mean texture values for the three different slabs are shown in Figure 27.

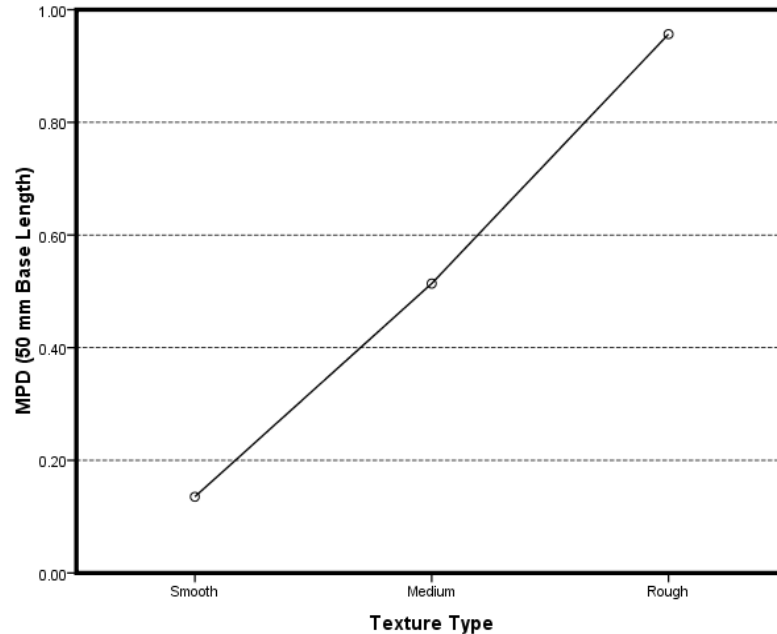


**FIGURE 27** Average MPD values for three different texture types, based upon 50 mm (2 inch) segment lengths.

The cores extracted from the pavements were examined to study the effect of traffic direction on the AIMS measurements. ANOVA analysis at a 0.05 significance level was performed on RMS values of each of the AIMS scanline directions shown in Figure 22. Figure 28 shows the relationship between mean RMS for a given specimen and the  $MPD_{\text{field}}$  value measured by CT Meter for that section. Figure 28 indicates that there is a strong relationship between CT Meter measured  $MPD_{\text{field}}$  and calculated laboratory RMS values. Mean RMS for a specimen was calculated by taking the average of the RMS values of four directions for that specimen.

The results of analysis showed that the RMS values of scans performed in different directions on the same sample are statistically different, as shown in Figure 29. Directional difference in texture occurs due to the polishing effect of passing traffic in which the macrotexture along the traffic direction is less than the macrotexture perpendicular to the traffic direction. Further statistical analysis of each direction pair by Tamhane post hoc analysis in SPSS (59) revealed that at least three independent directional measurements are required to obtain the macrotexture of field cores. Tamhane's test is a post hoc test suitable for comparing means of different populations when the homogeneity of variances assumption is not met (59). Statistical analysis using ANOVA showed that there is no significant difference between MPDs calculated from scanlines in four directions and MPDs calculated from scanlines in three directions; and any set of three measurements can be used to find the MPD values.

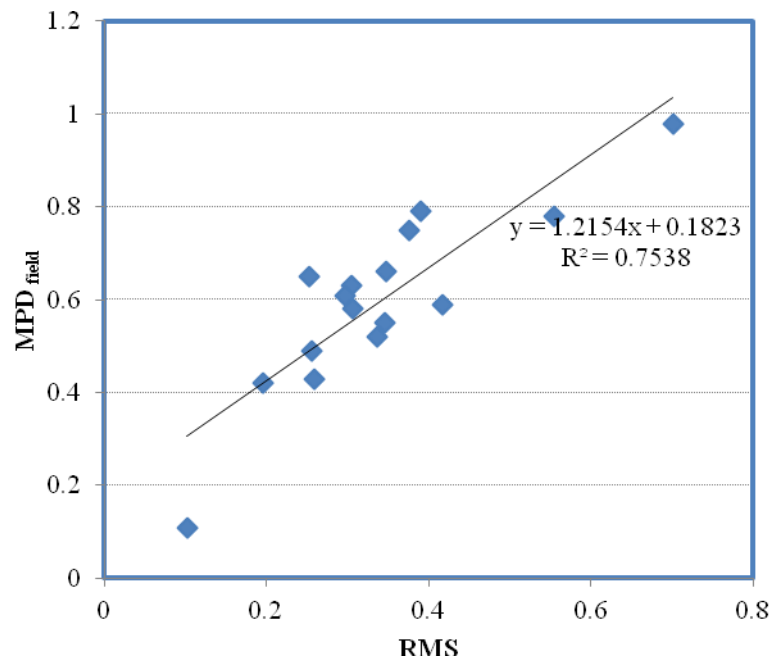


**FIGURE 28 Relationship between mean RMS from AIMS and field (CT Meter) MPD.**

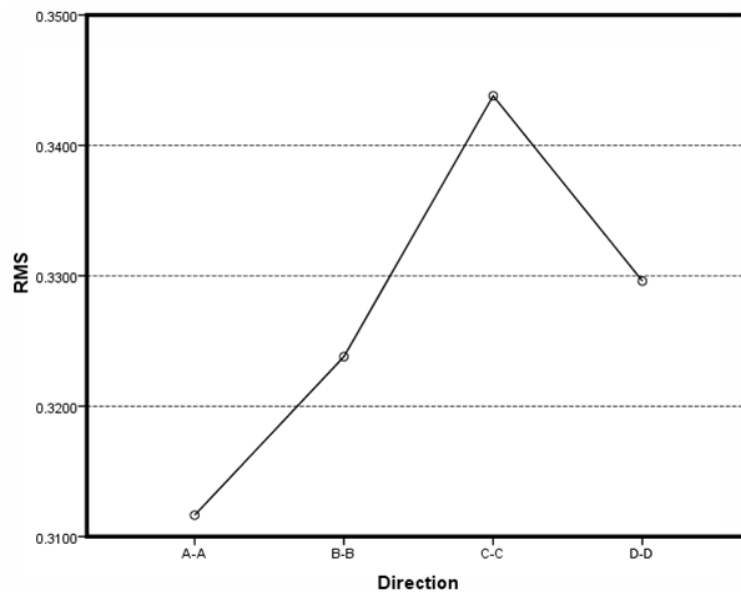


**FIGURE 29 Mean AIMS RMS values by direction of scanline.**

## CONCLUSIONS

The aggregate imaging system (AIMS) is a useful tool for measuring the shape characteristics of aggregates. Another application of this equipment is to measure pavement core texture. In this research study, the feasibility of using the AIMS equipment for roadway macrotexture measurement from pavement cores was investigated and shown to be useful. Macrotexture was measured on 13 field cores and nine small slab samples from fabricated concrete slabs. The fabricated slabs were negative images of actual field pavements cast with Portland cement concrete. The macrotexture of the fabricated slabs ranged from smooth to rough. Each small slab specimen was scanned in four different directions, and each scanline was divided into segments with three different segment lengths (75 mm (3 inch), 50 mm (2 inch), and 25 mm (1 inch)). MPD values for each small slab sample were calculated by picking the highest peak in each segment and averaging all of the segment peak heights for each specimen.

Statistical analysis showed that there is good correlation between the MPD values from AIMS measurements calculated based on a 50 mm (2 inch) segment length and the MPD measured on the pavement in the field with the CT Meter. Therefore, a 50 mm (2 inch) segment length is recommended for calculating texture from AIMS measurements of cores or pavement texture samples. An equation was recommended for estimating field MPD values based on laboratory measurements.

Further analysis using RMS values showed that the proposed procedure using AIMS is sensitive to the direction of the scanlines and can therefore distinguish traffic direction. A set of three directional measurements can be used instead of four directional measurements, and the conclusions are still valid. The mean RMS values using AIMS also had a fairly strong relationship with the MPD values measured by the CT Meter and further support the use of AIMS to measure macrotexture.

## **FUTURE RESEARCH**

Further verification and refinement of the AIMS methodology proposed for measuring pavement texture in the laboratory is recommended. Only 19 samples were included in this study, and it is expected that additional study with more samples would result in more accurate refinement of the regression equation. Also, the predictive power of the procedure and the equations could be strengthened by including additional types of textures in the sampling.

## **6. SUMMARY OF CONCLUSIONS, RECOMMENDATIONS, AND FUTURE RESEARCH**

This section summarizes the following items from the previous sections of this thesis:

- Main results and findings of this research project;
- Corresponding recommendations of methods to be used for chip seal emulsion residue characterization and pavement macrotexture evaluation

Topics are included in the discussion that were not studied experimentally in this project but which could provide additional improvement of the proposed methodologies.

### **Conclusions and Recommendations: Emulsion Residue Testing and Characterization**

The following conclusions and recommendations have been made concerning emulsion residue testing and characterization in this thesis:

- Recovered emulsion residues were shown to be different from their base binders at high temperatures in the unaged state, but they were similar to their base binders at cold temperatures after aging (7).
- Recovered residues from the two recovery methods utilized in this project (the hot oven evaporation method and the stirred can with nitrogen purge method) were oxidized more than their base binders but at similar levels to each other (7).
- Surface Performance Grading (SPG), which uses the same equipment as that used in the Performance Graded (PG) system but with some procedural modifications and with different limiting values for the test parameters to account for differences in critical distress, aging conditions, and appropriate temperatures, is recommended as the performance graded specification for chip seal emulsion residues (7).



- A strawman emulsion residue specification based on that proposed from TxDOT research (14, 16) and modified based on the results of this project is proposed and is shown in Table 3 (7).
- Based on the methods evaluated in this project, the stirred can emulsion residue recovery method is recommended for use with the proposed specification (7).
- Additional work with another recovery method, the warm oven evaporative recovery, is ongoing and may replace the stirred can residue recovery as the recovery method of choice (20, 21, 22). The newer recovery method is expected to not disturb the structural matrix that develops upon emulsion breaking and water evaporation. Recoveries involving high heat may be breaking down the matrix which results from some of the polymeric additives.
- The thresholds provided in the strawman specification for the DSR and BBR parameters are based on validation with mostly Texas field sections. It is likely that they need further adjustment for climates in other parts of the country similar to the manner in which they were adjusted in this project (7).
- Strain sweeps performed with the DSR on curing and unaged emulsion residues are recommended to evaluate strain resistance and stiffness development. These tests could be used to predict when emulsion based chip seals will develop enough stiffness to be opened to traffic (7).
- Strain sweeps could also be used to assess a material's resistance to raveling, both in newly constructed chip seals and after the critical first seasons of weather and aging. Additional work is needed to verify the proper test parameters for the strain sweeps and to refine the performance criteria (7).
- The strain sweep thresholds included in the strawman specification were selected to reflect the significantly different performance of emulsion 3 and the Utah Arches emulsion 6 (7).

## **Conclusions and Recommendations: Pavement Macrotexture Evaluation**

The following conclusions and recommendations have been made concerning pavement macrotexture evaluation in this thesis:

- Based on the results from this project, this thesis recommends the use of the CT Meter for assessing existing pavement macrotexture for use in adjusting emulsion spray rate in a chip seal operation. The CT Meter is fairly portable, runs the macrotexture measurement quickly, and the MPD compares well to the standard of macrotexture measurement, the MTD from the sand patch test.
- There is a new and alternative laser texture measuring device, the Ames laser texture scanner, being investigated in other research (37, 48) which has been shown to produce acceptable macrotexture evaluations when compared to measurements made with the sand patch method and with the CT Meter. It is expected that the Ames device would be an effective alternative to the sand patch test and to the CT Meter for measuring pavement macrotexture, especially before a chip seal operation. The Ames device is very portable and less expensive than the CT Meter.
- The AIMS MPD also compared well in this research to the CT Meter MPD. However, the AIMS equipment is not currently portable and therefore requires samples to be brought into the laboratory. This is not practical for a chip seal operation.

## **Recommended Future Research**

The following future work is recommended as an outcome of the work done for this thesis:

- Further performance monitoring of the three chip seal projects constructed and studied in this project is recommended (7).

- Further field validation and refinement of the grading criteria of the SPG grading system is recommended (7).
- Extension of the SPG criteria to regions other than Texas needs to be pursued (7).
- Further research and refinement of strain sweep testing on the DSR for evaluation of emulsion residue resistance to permanent deformation is recommended (7).
- Cold temperature testing using the BBR needs to be replaced with an alternative test which measures  $G^*$  at cold temperatures directly. Research being done at University of Wisconsin Madison and at Western Research Institute (29) may produce a replacement test. It will be important to include the findings in the SPG emulsion residue grading system (7).
- Further evaluation of the emulsion residue recovery methods which includes the warm oven evaporative method to determine which produces residue that most closely simulates emulsion residue in the field is recommended (7).
- Evaluation of the Ames laser texture meter for use in pavement macrotexture evaluation on chip seal projects is recommended.
- It is suggested that, if the AIMS profiling technique could be developed within a portable device, this could be effectively used for macrotexture measurement on chip seal construction sites. However, one issue with this might be that the profiling would take too long to be safe for the technician taking the measurement on the roadway. Also, these measurements would often be taken in front of the chip sealing operation and would need to be rapid.
- A portable camera system could be developed which uses wavelet transform analysis of grayscale images for evaluating pavement macrotexture, instead of fast Fourier transform analysis of black and white images as has been developed elsewhere for measuring chip seal roughness (49). Such a system could provide a viable, rapid, and relatively inexpensive alternative to the sand patch test MTD and the CT Meter MPD for rapid measurement and analysis in the field of pavement macrotexture.

- Two of the methods for measuring pavement texture that were recommended in this thesis for future research have the potential for making field measurements of microtexture in addition to macrotexture. These methods are a portable camera system which measures texture using the wavelet transform analysis of grayscale images and the Ames laser texture scanner. These need to be further investigated because there is currently no method for measuring pavement microtexture in the field.

## REFERENCES

1. Shuler, S., A. Lord, A. Epps Martin, D. Hoyt. *Manual for Emulsion-Based Chip Seals for Pavement Preservation*. NCHRP Report 680. Transportation Research Board of the National Academies, Washington, D.C., 2011.
2. Federal Highway Administration. *Pavement Preservation, A Roadmap for the Future: Ideas, Strategies, and Techniques for Pavement Preservation*. A Forum Held in Kansas City, Missouri, October 26-28, 1998. Online at <http://www.fhwa.dot.gov/infrastructure/asstmgmt/roadmap.pdf>, last accessed on 9/27/2011.
3. Texas Department of Transportation. *Seal Coat and Surface Treatment Manual*. Revised May 2010. Online at <http://onlinemanuals.txdot.gov/txdotmanuals/scm/scm.pdf>, last accessed on 9/30/2011.
4. Wood, T.J., D.W. Janisch, and F.S. Gaillard. *Minnesota Seal Coat Handbook 2006*. Project Report MN/RC - 2006-34. Minnesota Department of Transportation, June, 2006. Online at <http://www.lrrb.org/pdf/200634.pdf>, last accessed on 9/30/2011.
5. Stevenson, J. *Maintenance Chip Seal Manual*. Montana Department of Transportation, 1996.
6. *Performance Graded Asphalt Binder Specification and Testing*. Superpave Series No. 1 (SP-1). Asphalt Institute, Lexington, Kentucky, Undated.
7. Hoyt, D., A.E. Martin, and S. Shuler. Surface Performance-Grading System to Grade Chip Seal Emulsion Residues. In *Transportation Research Record: Journal of the Transportation Research Board, No. 2150*. Transportation Research Board of the National Academies, Washington, D.C., 2010, pp. 63-69.
8. Rezaei, A., D. Hoyt, and A.E. Martin. Simple Laboratory Method for Measuring Pavement Macrotecture: Pavement Cores and Aggregate Image Measurement System. In *Transportation Research Record: Journal of the Transportation Research*

- Board, No. 2227.* Transportation Research Board of the National Academies, Washington, D.C., 2011, pp. 146-152.
9. Freemantle, M. What's That Stuff? *Chemical and Engineering News*, Volume 77, Number 47, November 22, 1999. Online at <http://pubs.acs.org/cen/whatstuff/stuff/7747scit6.html>, last accessed 8/21/2011.
  10. Sebaaly, P. Rheological Properties of Polymer-Modified Asphalt Binders. *Asphalt Science and Technology*. Edited by A.M. Usmani. Marcel Dekker Inc., New York, 1997, pp. 235-247.
  11. Bahia, H. Modeling of Asphalt Binder Rheology and Its Application to Modified Binders. *Modeling of Asphalt Concrete*. Edited by Y. Kim, ASCE Press, New York, 2009, pp. 11-61.
  12. Anderson, D., and T.W. Kennedy. Development of SHRP Binder Specification. *Journal of the Association of Asphalt Paving Technologists*, Volume 62, 1993, pp. 481-507.
  13. Roberts, F., P.S. Kandhal, E. R. Brown, D.Y. Lee, and T.W. Kennedy. *Hot Mix Asphalt Materials, Mixture Design, and Construction*. Second Edition. National Asphalt Pavement Association Research and Education Foundation, Lanham, Maryland, 1996.
  14. Epps, A.L., C.J. Glover, and R. Barcena. *A Performance-Graded Binder Specification for Surface Treatments*. Report No. FHWA/TX-02/1710-1. Texas Department of Transportation and U.S. Department of Transportation, FHWA, 2001.
  15. Walubita, L.F., A.E. Martin, and C.J. Glover. *A Surface Performance-Graded (SPG) Specification for Surface Treatment Binders: Development and Initial Validation*. Report No. FHWA/TX-05/0-1710-2. Texas Department of Transportation and Federal Highway Administration, U.S. Department of Transportation, 2005.
  16. Barcena, R, A. Epps Martin, and D. Hazlett. Performance Graded Binder Specification for Surface Treatments. In *Transportation Research Record: Journal of the Transportation Research Board, No. 1810*. Transportation Research Board of the National Academies, Washington D.C., 2002, pp. 63-71.

17. *Pavement Preservation Concepts and Techniques*. FHWA Publication No. FHWA-RC-BAL-04-0015. Federal Highway Administration, Washington, D.C., 2004.
18. Walubita, L.F., A. Epps Martin, D. Hazlett, and R. Barcena. Initial Validation of a New Surface Performance-Graded Binder Specification. In *Transportation Research Record: Journal of the Transportation Research Board*, No. 1875. Transportation Research Board of the National Academies, Washington D.C., 2004, pp. 45-55.
19. ASTM D244-97C. *Standard Test Methods and Practices for Emulsified Asphalts*. ASTM International, Conshohocken, Pennsylvania, 1997.
20. ASTM D7497-09. *Standard Practice for Recovering Residue from Emulsified Asphalt Using Low Temperature Evaporative Techniques*. ASTM International, Conshohocken, Pennsylvania, 2009.
21. Kadrmas, A. Report on Comparison of Residue Recovery Methods and Rheological Testing of Latex and Polymer Modified Asphalt Emulsions. Report #4-AEMA ISAET 08. Presented at the Annual Meeting of the American Emulsion Manufacturers Association, Arlington, Virginia, 2008.
22. Hanz, A., Z. A. Arega, and H. U. Bahia. Rheological Evaluation of Emulsion Residues Recovered Using Newly Proposed Evaporative Techniques. Paper #09-2877. Presented at the Transportation Research Board 88<sup>th</sup> Annual Meeting, Washington, D.C., January 2009.
23. Prapaitrakul, N., R. Han, X. Jin, A. Epps Martin, and C. Glover. Comparative Study on Recovered Binder Properties Using Three Asphalt Emulsion Recovery Methods. *Journal of Testing and Evaluation*, Volume 38, Number 6, November 2010, pp. 70-76.
24. Kucharek, A. Measuring the Curing Characteristics of Chip Sealing Emulsions. Asphalt Emulsion Manufacturers Association and McAsphalt, Scarborough, Ontario. Presented at the Joint ARRA-ISSA-AEMA Meeting, Bonita Springs, California, 2007.

25. ASTM D7000 – 08. *Standard Test Method for Sweep Test of Bituminous Emulsion Surface Treatment Samples*. ASTM International, Conshohocken, Pennsylvania, 2009.
26. Woo, J.W., E. Ofori-Abebesse, A. Chowdhury, J. Hilbrich, Z. Kraus, A. Epps Martin, and C. Glover. *Polymer Modified Asphalt Durability in Pavements*. Report #FHWA/TX-07/0-4688-1, Texas Transportation Institute, College Station, Texas, November 2006.
27. *LTPP Seasonal Asphalt Concrete (AC) Pavement Temperature Models*. Report No. FHWA-RD-97-103. Federal Highway Administration, U.S. Department of Transportation, Washington, D.C., 1997.
28. LTPPBIND, Version 3.0/3.1. Federal Highway Administration, U.S. Department of Transportation, Washington, D.C. Online at <http://www.fhwa.dot.gov/PAVEMENT/ltppltppbind.cfm>, page modified 2009, last accessed 1/2010.
29. Pavement Preservation Emulsion Task Force Meeting Minutes. Lexington, Kentucky, December, 2008. Online at [http://www.asphaltinstitute.org/ai\\_pages/Technical\\_Focus\\_Areas/ETG\\_Minutes\\_Agendas/Pavement\\_Preservation ETF\\_Meeting\\_Minutes\\_12\\_15\\_08.pdf](http://www.asphaltinstitute.org/ai_pages/Technical_Focus_Areas/ETG_Minutes_Agendas/Pavement_Preservation ETF_Meeting_Minutes_12_15_08.pdf), last accessed 11/8/2009.
30. Hall, J.W., K.L. Smith, L. Titus-Glover, J.C. Wambold, T.J. Yager, and Z. Rado. *Guide for Pavement Friction*. Final Report, Project 1-43. National Cooperative Highway Research Program, Transportation Research Board, Washington, D.C., 2006.
31. ASTM E 965-96 (Reapproved 2006). *Standard Test Method for Measuring Pavement Macrotexture Depth Using a Volumetric Technique*. Volume 04.03. ASTM International, Conshohocken, Pennsylvania, 2006.
32. ASTM E 2157-01 (Reapproved 2005). *Standard Test Method for Measuring Pavement Macrotexture Properties Using the Circular Track Meter*. Volume 04.03. ASTM International, Conshohocken, Pennsylvania, 2005.



33. Abe, H., T. Akinori, J.J. Henry, and J. Wambold, Measurement of Pavement Macrottexture with Circular Texture Meter. In *Transportation Research Record, Journal of the Transportation Research Board, No. 1764*. Transportation Research Board of the National Academies, Washington, D. C., 2001, pp. 201-209.
34. Hanson, D.I. and B.D. Prowell. *Evaluation of Circular Texture Meter for Measuring Surface Texture of Pavements*. NCAT Report 04-05. National Center for Asphalt Technology, Auburn, Alabama, 2004.
35. Alderson, A. *Update of the Austroads Sprayed Seal Design Method*. Austroads Technical Report AP-T68/06. Austroads, Inc., Sydney, Australia, 2006.
36. South African National Roads Agency. *Design and Construction of Surfacing Seals*. Technical Recommendations for Highways, TRH 3, Pretoria, Republic of South Africa, May 2007.
37. Sezen, H., N. Fisco, and P. Luff. *Validation of ODOT's Laser Macrottexture System*. Executive Summary Report FHWA/OH-2008/12. The Ohio Department of Transportation Office of Research and Development, Columbus, Ohio, 2008.
38. Nippo Sangyo Co., Ltd. Circular Texture Meter Product Guide. Online at <http://www.nippou.com/en/products/ct.html>, last accessed on 9/12/11.
39. ASTM E 1845-01. *Standard Practice for Calculating Pavement Macrottexture Mean Profile Depth*. Volume 04.03. ASTM International, Conshohocken, Pennsylvania, 2003.
40. Masad, E. *Aggregate Imaging System (AIMS): Basics and Applications*. Implementation Report FHWA/TX-05/5-1707-01-1, Texas Transportation Institute, College Station, Texas, 2005.
41. MathWorks. *MathWorks Product Documentation*. Online at <http://www.mathworks.com/help/toolbox/images/f11-27972.html>, last accessed on 9/14/2011.
42. Masad, E. *The Development of a Computer Controlled Image Analysis System for Measuring Aggregate Shape Properties*. NCHRP-IDEA Project 77 Final Report.

- National Cooperative Highway Research Program. Transportation Research Board, National Research Council, Washington, D.C., 2003.
43. Al Rousan, T.M. *Characterization of Aggregate Shape Properties Using a Computer Automated System*. PhD Dissertation, Texas A&M University, College Station, Texas, December, 2004.
  44. Gudimettla, J., L.A. Myers, and C. Paugh. *AIMS: The Future in Rapid, Automated Aggregate Shape and Texture Measurement*. Federal Highway Administration, Washington, D.C. Online at [http://www.pineinst.com/test/pdf/FHWA\\_Gudimettla-Myers-Paugh.pdf](http://www.pineinst.com/test/pdf/FHWA_Gudimettla-Myers-Paugh.pdf), last accessed 9/20/2011.
  45. Mallat, S. *A Wavelet Tour of Signal Processing*, Second Edition. Academic Press, San Diego, 1999.
  46. Ames Engineering. Description of Model 9200 Laser Texture Scanner. Ames, Iowa. Online at <http://www.amesengineering.com/TextureScanner.html>, last accessed 1/18/2012.
  47. Ames Engineering. *Ames Engineering Laser Texture Scanner User Manual*. Ames, Iowa, 2008.
  48. Fisco, N. *Comparison of Macrottexture Measurement Methods*. M.S. Thesis, The Ohio State University, Columbus, Ohio, 2009.
  49. Pidwerbesky, B., J. Waters, D. Gransberg, and R. Stemprok. *Road Surface Texture Measurement Using Digital Image Processing and Information Theory*. Research Report 290. New Zealand Land Transport Agency, Wellington, New Zealand, 2006.
  50. Henry, J. *Evaluation of Pavement Friction Characteristics: A Synthesis of Highway Practice*. NCHRP Synthesis 291. National Cooperative Highway Research Program, Transportation Research Board, Washington, D.C., 2000.
  51. Dewey, G.R., A.C. Robords, B.T. Armour, and R. Muethel. Aggregate Wear and Pavement Friction. Presented at the Transportation Research Board 80th Annual Meeting, Washington, D.C., 2001.

52. Noyce, D., H. Bahia, J. Yambo, and G. Kim. *Incorporating Road Safety into Pavement Management: Maximizing Asphalt Pavement Surface Friction for Road Safety Improvements*. Final Report. Midwest Regional University Transportation Centre, Madison, Wisconsin, June, 2007.
53. Linder, M., M. Kröger, K. Popp, and H. Blume. *Experimental and Analytical Investigation of Rubber Friction*. International Congress of Theoretical and Applied Mechanics, Warsaw, Poland, 2004.
54. Fletcher, T., C. Chandan, E. Masad, and K. Sivakuma. Aggregate Imaging System for Characterizing the Shape of Fine and Coarse Aggregates. In *Transportation Research Record: Journal of the Transportation Research Board*, No. 1832, Transportation Research Board of the National Research Council, Washington, D.C., 2003, pp. 67-77.
55. *Pavement Selection for City Streets*. Texas Asphalt Pavement Association. Technical Article, June 16, 2005. Online at [http://www.txhotmix.org/public\\_articles.php?article\\_id=6&](http://www.txhotmix.org/public_articles.php?article_id=6&), last accessed July 30, 2010.
56. Masad, E.A., D. Little, L. Tashman, S. Saadeh, T. Al-Rousan, and R. Sukhwani. *Evaluation of Aggregate Characteristics Affecting HMA Concrete Performance*. Research Report ICAR 203-1. Texas Transportation Institute, College Station, Texas, 2003.
57. Masad, E. *The Development of a Computer Controlled Image Analysis System for Measuring Aggregate Shape Properties*. National Cooperative Highway Research Program NCHRP-IDEA, Project 77 Final Report, Transportation Research Board, National Research Council, Washington, D.C. 2003.
58. *Aggregate Imaging Measurement System: Model AFA2A Operation Manual*. Pine Instrument Company, Grove City, Pennsylvania, March, 2010.
59. *SPSS Graduate Pack 16.0 for Windows*. Statistical Program for the Social Sciences. SPSS Inc., Chicago, Illinois, 2007.

60. Borgatti, S.P. The Root Mean Square. Online at  
<http://www.analytictech.com/mb313/rootmean.htm>. Copyright 1996-98, Revised.  
Last Accessed 9/12/2011.

**VITA**

Name: Denise Marie Hoyt

Address: CE/TTI 310  
3136 TAMU  
College Station, TX 77843-3136  
USA

Email Address: phoenixdeni@yahoo.com

Education: Associate's Degree, Land Surveying, Community College of  
Denver, 1978  
B.S., Civil Engineering, Texas A&M University, 1984

Research Interests: Testing and Characterization of Bituminous Materials; Macrotexture,  
Friction, and Drainage Testing of Pavements